RESULTS

The NF-κB-activating Tax–HSP90–IKK ternary complex is disaggregated by HSP90 inhibitors that induce Tax degradation

The molecular chaperone HSP90 and its co-chaperone CDC37 are both recruited to IKK and play essential roles in TNF-α-triggered HMW-IKK formation and subsequent NF-κB activation. The addition of the HSP90-specific inhibitor GA completely suppresses NF-κB signaling.[12] As we previously demonstrated that the expression of Tax also resulted in the formation of a HMW-IKK complex for activating NF-κB,[11] we speculated that the inhibition of HSP90 function by GA would also affect Tax-mediated NF-κB signaling. First, using Tax-expressing MT4 cells, we confirmed the interaction of Tax with HSP90 in the same protein complex by Co-IP assays (Figure 1a). We then treated MT4 cells for 24 h with a newly developed, less toxic and water-soluble GA derivative, 17-DMAG,[22] to evaluate its effects on the formation of a Tax-induced ternary complex, Tax–HSP90–IKK. To our surprise, the amount of Tax in MT4 cells decreased progressively with increasing doses of 17-DMAG (Figure 1b, upper panel) despite no apparent changes in the amount of HSP90 in the same lysate (data not shown). Under these conditions, the interaction between HSP90 and IKKβ was clearly reduced with increasing doses of 17-DMAG (Figure 1b, middle panel), whereas the amount of HSP90 immunoprecipitated throughout this range of concentrations was unchanged (Figure 1b, lower panel).

We then examined the kinetics of Tax degradation in MT4 cells treated with 17-DMAG. Reductions in Tax levels were observed in cells treated for 12 h and continued over time until by 48 h, when the level of Tax became undetectable (Figure 1c). This 17-DMAG-induced Tax degradation stabilized I κBα, whereas another NF-κB inhibitor dexamethasone had no effects (Supplementary Figure 1). Tax degradation by 17-DMAG occurred prior to mRNA suppression as the marked decrease of Tax mRNA was not observed until 24 h after treatment (Figure 1d), whereas protein level of Tax was obviously decreased by 12 h (compare Figures 1c and d). Our previous study indicated that Tax degradation is partly induced by caspase,[30] and polyubiquitylation had little effects on its cellular stability.[31] We therefore re-evaluated which pathway is responsible for the 17-DMAG-induced Tax degradation (Figure 1e). Tax degradation was partly blocked by the caspase inhibitor zVAD-fmk[30] and by autophagy inhibitors 3-methyladenine (3-MA) and 5-aminoimidazole-4-carboxamide-1-b-D-ribofuranoside (AICAR)[32] but not by the proteasome inhibitor MG132. Similar findings were obtained from parallel studies using another ATL cell line, C8166 (data not shown), although more investigation is needed for fully understanding of Tax instability.

GA and its derivatives are known to suppress a variety of intracellular signaling pathways, including NF-κB activation by inhibiting IKK.[12,33] One of the most important functions of NF-κB is to protect cells from apoptotic stress. A portion of 2.5 μM of 17-DMAG is sufficient to induce Tax degradation (Figure 1c) and I κBα stabilization (Supplementary Figure 1), which implies the suppression of ATL cell growth; however, it is important to know whether this concentration is toxic to normal PBLs. We, therefore, confirmed the median inhibitory concentrations of 17-DMAG for several ATL or non-ATL cell lines along with normal PBLs.

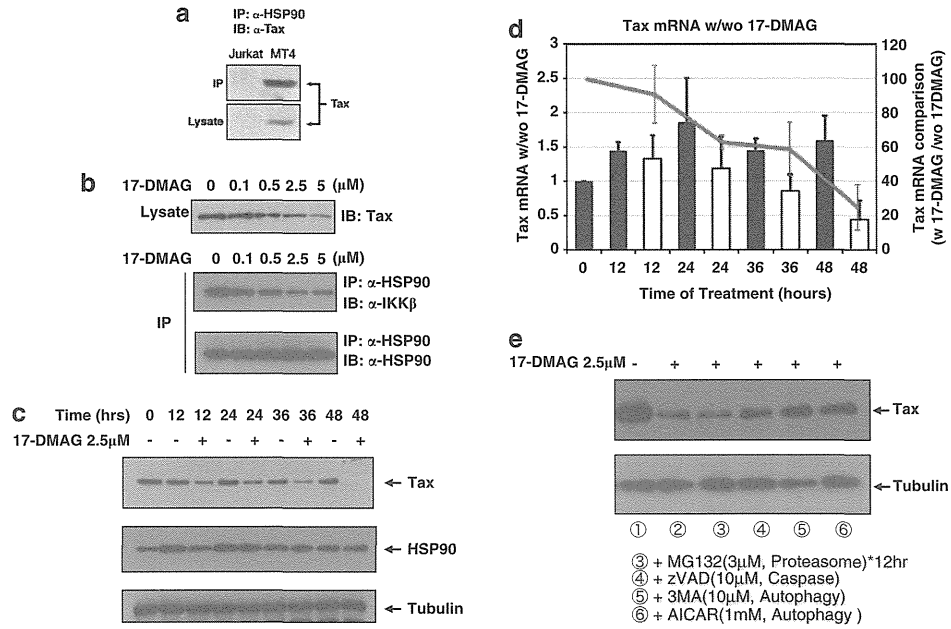

Figure 1. 17-DMAG inhibits HSP90–Tax–IKK ternary complex formation and induces Tax degradation in ATL cells. (**a**) Co-IP of Tax and HSP90. Four million Jurkat or MT4 cells were lysed with Co-IP buffer, and 50 μg total of cell lysates were subjected to IP with 2 μg of rabbit polyclonal anti-HSP90 antibody, followed by immunoblot (IB) with mouse monoclonal anti-Tax antibody (upper panel). The amount of expressed Tax in each cell line was verified by IB with anti-Tax against 10 μg of cell lysates (lower panel). (**b**) 17-DMAG's effects on Tax expression level and physical interaction between HSP90 and IKKβ in MT4 cells. Four million MT4 cells were treated with the indicated concentrations of 17-DMAG for 16 h. Co-IP and IB against immunoprecipitates or lysates were carried out as in panel **a**. (**c**) Ten micrograms of each cell lysate from MT4 cells treated with or without 2.5 μM of 17-DMAG for the indicated periods were subjected to sodium dodecyl sulfate-polyacrylamide gel electrophoresis, and Tax (upper panel), HSP90 (middle panel) or tubulin (lower panel) expression was detected using monoclonal anti-Tax, anti-HSP90 or anti-tubulin antibodies. (**d**) Expression levels of Tax in 17-DMAG-treated MT4 cells. mRNAs were prepared from the same aliquots of MT4 cells described in panel **c**. mRNAs from 17-DMAG-untreated fractions (black bars) and 17-DMAG-treated fractions (2.5 μM, white bars) with indicated time courses were analyzed with the universal probes (Roche) and primers through the LightCycler PCR method according to the manufacturer's direction. Comparison of Tax mRNAs with or without 17-DMAG was also indicated with a red line graph as a division of Tax mRNA with 17-DMAG/without 17-DMAG at each time point. (**e**) Four million MT4 cells were treated with 2.5 μM 17-DMAG for 24 h (lanes 2–6) and then additional 3 μM MG132 for 12 h (lane 3), 10 μM zVAD-fmk (lane 4) and 3-MA (lane 5) and 1 mM AICAR (lane 6) for 24 h. Lysates were prepared for IB of Tax and tubulin.

The median inhibitory concentrations to ATL cells vary from 0.06 to 2.33 μM, which is much lower than that of non-ATL Jurkat cells (9.32 μM), and three PBLs did not show any significant growth suppression with 10 μM of 17-DMAG (Supplementary Figure 2). We set the concentration of 17-DMAG at 2.5 μM and measured the effects on the viability of ATL cells (cell lines established from ATL patients' PBLs or cord blood cocultured with ATL patients' PBLs or primary PBLs of ATL patients) and other leukemic cells, as well as PBLs from HTLV-1-negative controls. Most of the ATL cell lines treated with 17-DMAG exhibited a rapid decrease in viability, whereas normal PBLs were unaffected by the drug (Figure 2a). 17-DMAG treatment also resulted in a marked increase in caspase-3/7 activity in most of the ATL cell lines while having no significant caspase perturbation in control PBLs (Figure 2b).

Downregulation of Tax occurs at the post-transcriptional stage

We then proceeded to examine the details of 17-DMAG-dependent inhibitory effects on the Tax–HSP90–IKK ternary complex by transfection of two different Tax expression vectors into HEK293 cells. One was driven by the simian virus 40 early promoter and

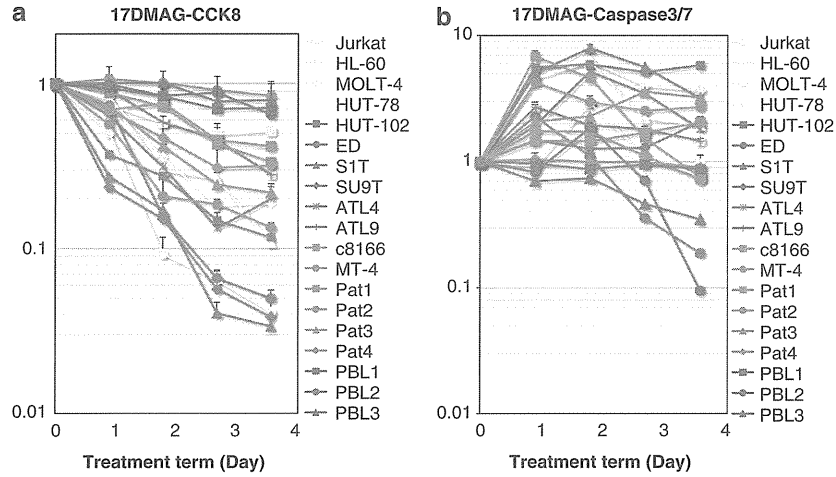

Figure 2. 17-DMAG induces growth arrest and apoptosis in ATL cells. Two million cells from each ATL cell line established from ATL patients' PBLs (HUT-102, ED, S1T, SU9T, ATL4 and ATL9; red lines), ATL cell lines established by coculture of cord blood and ATL patients' PBLs (C8166 and MT4; orange lines), PBLs from ATL patients (Pat1 to Pat4; purple lines), non-ATL leukemic cell lines (Jurkat, HL-60, MOLT-4 and HUT-78; yellow lines) or healthy donors (PBL1, PBL2 and PBL3; blue lines) were treated with 2.5 μM of 17-DMAG for 1–4 days. After each 24 h incubation, 10^4 (**a**) or 5×10^3 (**b**) cells were transferred to each well of a 96-well plate. (**a**) One-tenth volume of Cell Counting Kit 8 solution (Dojindo) was added to each fraction. Thirty minutes after incubation, the absorbance at 465 nm was measured using an E-max precision microplate reader (Molecular Devices Japan Co. Ltd., Tokyo, Japan). (**b**) The same volume of Apo-ONE homogeneous Caspase-3/7 assay solution was added to cells, and chemical luminescence was quantified with GloMax luminometer (Promega).

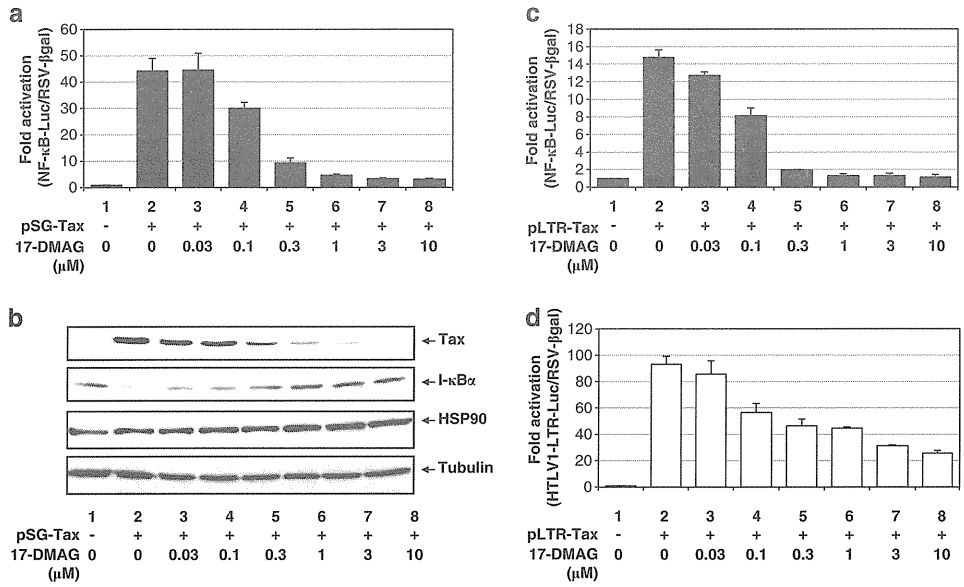

Figure 3. 17-DMAG downregulates all the Tax-mediated signaling in HEK293 cells. Fifty thousand HEK293 cells in each well on a 12-well plate were transfected with 0.5 μg of pSG-Tax (**a**, **c**) or pLTR-Tax along with 50 ng of NF-κB-luciferase (**a**, **c**) or HTLV-1-LTR-luciferase (**d**) and 50 ng of RSV-β-galactosidase control plasmid. A portion of 0.1–5 μM of 17-DMAG was added as indicated for 16 h. (**b**) The expression levels of Tax, HSP90 and tubulin in 10 μg of lysates from panel (**a**) were monitored by IB with monoclonal antibodies for each protein.

β-globin intron II (pSG5-Tax),[24] whereas the other was driven by the HTLV-1-LTR (LTR-Tax). These lines were transfected with either a NF-κB-responsive or a HTLV-1-LTR luciferase reporter (Figures 3a and b and Figures 3c and d, respectively) and RSV-β-galactosidase for readout normalization. 17-DMAG treatment was found to suppress Tax-mediated NF-κB (Figures 3a, b and c) or HTLV-1-LTR activation (Figure 3d) regardless of whether Tax was expressed from pSG5-Tax (Figures 3a and b) or LTR-Tax (Figures 3c and d). In these experiments, the ectopically expressed Tax from transfected plasmid was again downregulated by 17-DMAG (Figure 3b). The same results were also obtained from the cell lysates transfected with LTR-Tax or CMV-Tax (data not shown). In addition to these two enhancers, activator protein 1 activation by Tax[34] was also inhibited by 17-DMAG (data not shown). As the three discrete pathways

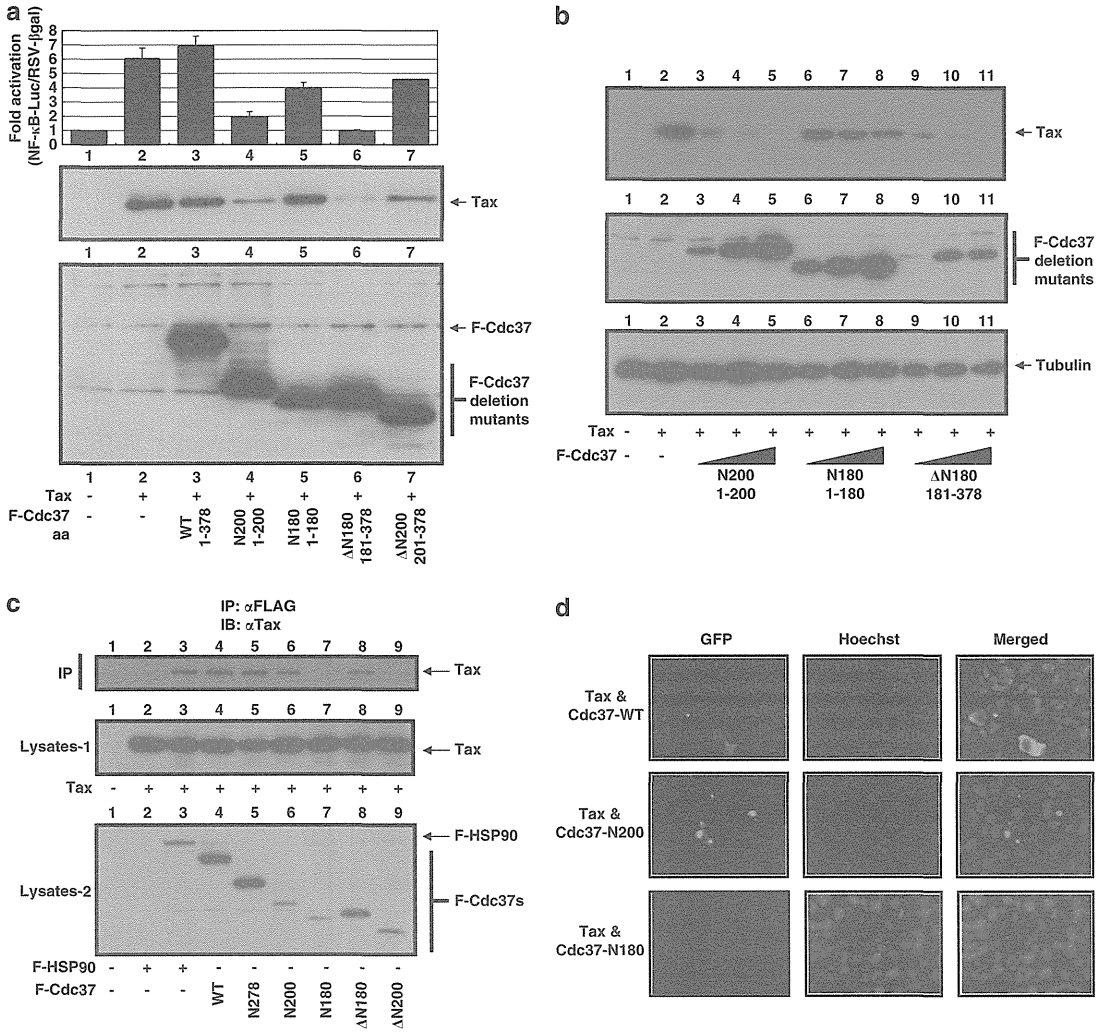

Figure 4. CBD of Cdc37 plays a crucial role for Tax stability in cells. (**a**) Co-transfection of LTR-Tax and pcDNA3-Flag-tagged Cdc37 (F-Cdc37) mutants. Lane 1: control pcDNA3 1 μg; lane 2: LTR-Tax 0.5 μg + pcDNA3 0.5 μg; lane 3: LTR-Tax 0.5 μg + F-Cdc37(1–378) wild type 0.5 μg; lane 4: LTR-Tax 0.5 μg + F-Cdc37(1–200) 0.5 μg; lane 5: LTR-Tax 0.5 μg + F-Cdc37(1–180) 0.5 μg; lane 6: LTR-Tax 0.5 μg + F-Cdc37(181–378) 0.5 μg; lane 7: LTR-Tax 0.5 μg + F-Cdc37(201–378) 0.5 μg. After 40 h transfection, HEK293 cells were lysed with 100 μl of lysis buffer, and the NF-κB-dependent luciferase activity was normalized with β-galactosidase value (upper panel). A portion of 10 μg of each lysate was resolved by sodium dodecyl sulfate-polyacrylamide gel electrophoresis, and the expression of Tax (middle panel) or Flag-tagged Cdc37s (lower panel) was detected by specific monoclonal antibodies. (**b**) Dose-dependent degradation of Tax by F-Cdc37 mutants. Lane 1: control pcDNA3 1 μg; lanes 2–11: 0.5 μg of LTR-Tax; lanes 3–5: plus 0.125, 0.25 and 0.5 μg of F-Cdc37(1–200); lanes 6–8: plus 0.125, 0.25 and 0.5 μg of F-Cdc37(1–180); lanes 9–11: plus 0.125, 0.25 and 0.5 μg of F-Cdc37(181–378). pcDNA3 was added to normalize the DNA amount. Tax (upper panel), Flag-tagged Cdc37s (middle panel) and tubulin (lower panel) were detected by specific monoclonal antibodies. (**c**) Cdc37's CBD (amino-acid residues 181–200(ref. 26)) is required for Tax interaction. A portion of 0.5 μg of control pcDNA3 (lane 1) or LTR-Tax (lanes 2–9) was transfected (lysate-1, middle panel) and 0.5 g of control pcDNA3 (lanes 1 and 2), F-HSP90 (lane 3), wild-type F-Cdc37(1–378, lane 4), F-Cdc37(1–278, lane 5), F-Cdc37(1–200, lane 6), F-Cdc37(1–180, lane 7), F-Cdc37(181–378, lane 8) and F-Cdc37(201–378, lane 9) were transfected separately (lysate-2, lower panel). The expression of each protein in cell lysates was detected by specific monoclonal antibodies (middle and bottom panels). A portion of 200 μg of each lane's cell lysates was mixed and subjected to Co-IP with 2 μg of rabbit anti-Flag antibodies, and each Co-IP complex was washed four times with Co-IP buffer, and following sodium dodecyl sulfate-polyacrylamide gel electrophoresis, Tax was detected by anti-Tax antibody (upper panel). (**d**) GFP two-hybrid binding assay between Cdc37 and Tax. HEK293 cells seeded on the six-well plates were transfected with phmKGN-MC-Tax and phmKGC-MN-Cdc37 or its mutant −Cdc37(N200) and −Cdc37(N180) by FugeneHD. After 48 h incubation, the transfected HEK293 cells were treated with Hoechst 34442 (Sigma) at the final concentration of 1 μM. Light and fluorescent (GFP and Hoechst 34442) microscopic observation and photography were performed by BZ-9000 Biorevo all-in-one fluorescence microscope (Keyence).

activated by Tax are inhibited by 17-DMAG treatment, the simplest interpretation suggests that all these effects arise from 17-DMAG-mediated destabilization of the Tax protein itself.

The client-binding domain of CDC37 plays crucial roles in Tax stabilization and Tax-mediated NF-κB activation

The molecular chaperone activity of HSP90 is usually exerted in cooperation with various co-chaperones. CDC37 was identified along with HSP90 as an essential component for a TNF-α-activated HMW-IKK complex.[12] As our current study shows the involvement of HSP90 in Tax-mediated HMW-IKK formation and NF-κB activation,[11,17] we generated Flag-tagged serial deletion mutants of HSP90 and CDC37 to examine their potential effects on Tax activity.

HSP90 has three distinct functional domains as described in Supplementary Figure 3.[35–37] We generated five deletion mutants, N, N + M, M, M + C and C, and transduced each with a Tax expression vector into HEK293 cells to determine any dominant-negative effects. Surprisingly, none of these mutants showed suppressive effects on Tax-mediated NF-κB activation or Tax stabilization (data not shown).

We then investigated the possible involvement of CDC37 in Tax stabilization and NF-κB signaling according to its functional domains (Supplementary Figure 3), namely, an HSP90-binding domain expanding through M164 to E221;[38] a kinase-binding domain at amino-acid residues 40–110;[39] a client-binding domain (CBD, amino-acid residues 181–200);[26] and a self-dimerization domain (amino-acid residues 240–260).[39] Although overexpression of full-length CDC37 slightly enhanced NF-κB activation (Figure 4a upper panel, lane 3), the mutants containing CBD, CDC37(1–200) and CDC37(181–378), strongly suppressed Tax-mediated NF-κB activation (Figure 4a upper panel, lanes 4 and 6) and induced extensive Tax degradation (Figure 4a middle panel, lanes 4 and 6). The mutants CDC37(1–180) and CDC37 (201–378) lacking CBD had little effects on either NF-κB activation or Tax stability (lanes 5 and 7). Tax degradation was reconfirmed by titration of these mutants (Figure 4b). Both CCD37(1–200) and CCD37 (181–378) progressively promoted Tax degradation (lanes 3–5 and 9–11, respectively), but CDC37(1–180) had little effects (lanes 6–8). Coexpression of certain sets of CDC37 mutants could promote Tax degradation through impaired physical interaction with Tax. We transfected HEK293 cells with Tax or Flag-CDC37 expression vectors separately to avoid spontaneous Tax degradation, and each cell lysate was mixed and applied for Co-IP experiments with anti-Flag antibodies (Figure 4c). Each protein expression was confirmed by immunoblotting for Tax (middle panel) or Flag (lower panel). Although the immunoprecipitates from wild-type HSP90 (upper panel, lane 3), CDC37 (lane 4) and Tax-degrading CDC37(1–200) and CDC37(181–378) (lanes 6 and 8) contained Tax in the complex, the immunoprecipitates from CDC37(1–180) and CDC37(201–378) lacking Tax-degrading properties did not (lanes 7 and 9).

Finally, we examined direct interaction between the two proteins using a GFP two-hybrid assay. Tax, tagged with the N-terminal portion of Kusabira-Green[27] fluorescent protein, and CDC37s (1–378, 1–200 and 1–180), tagged with the C-terminal portion, were co-transfected into HEK293 cells. Consistent with Co-IP results, co-transfectants of Tax and CDC37(1–378) or CDC37(1–200) emitted green fluorescence but Tax plus CDC37

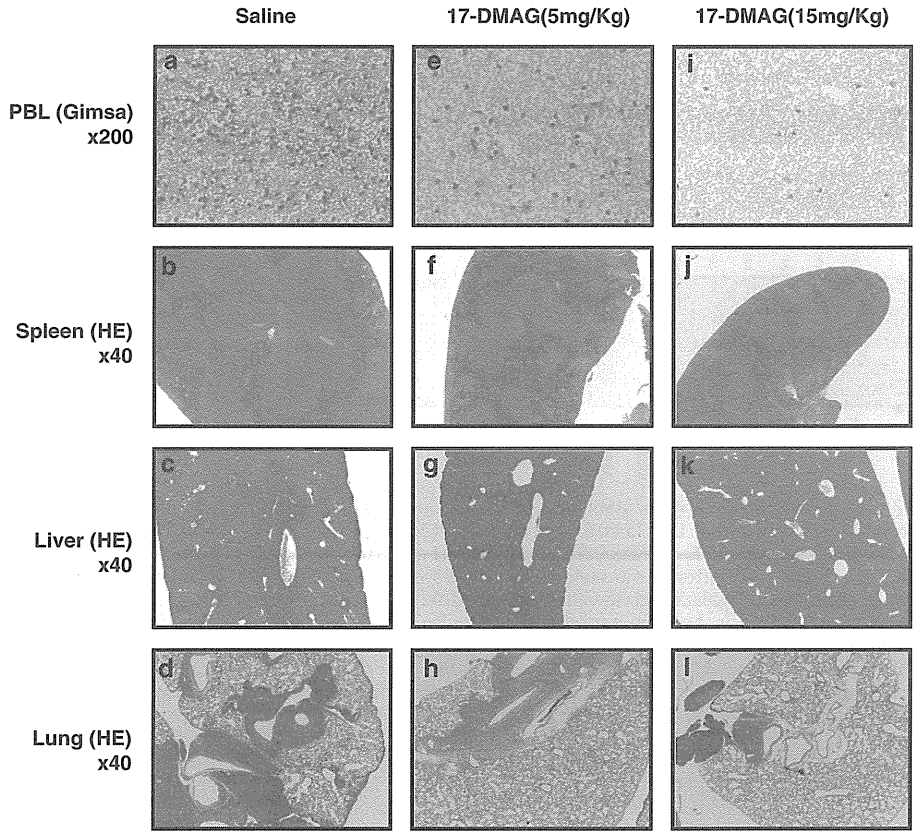

Figure 5. Oral administration of 17-DMAG blocks aggressive infiltration of Lck-Tax Tg cells into multiple organs of SCID mice. Two million Lck-Tax Tg cells were injected intraperitoneally into SCID mice. 17-DMAG was administered orally 5 days per week, with 5 mg/kg body weight (**e**–**h**) or 15 mg/kg body weight (**i**–**l**) or untreated (**a**–**d**). Mice were sacrificed after 21 days incubation, and organs were processed for Giemsa (**a**, **e**, **i**) or hematoxylin and eosin (HE, **b**–**d**, **f**–**h** and **j**–**l**) staining. Microscopic observations were performed and photographed with indicated magnifications. Tg, transgenic.

(1–180) did not. The Tax–CDC37(1–200) complex was translocated to the nucleus, whereas Tax–CDC37(1–378; wild type) stayed in the cytoplasm (Figure 4d). Collectively, these findings suggested the direct involvement of CDC37 for Tax stabilization.

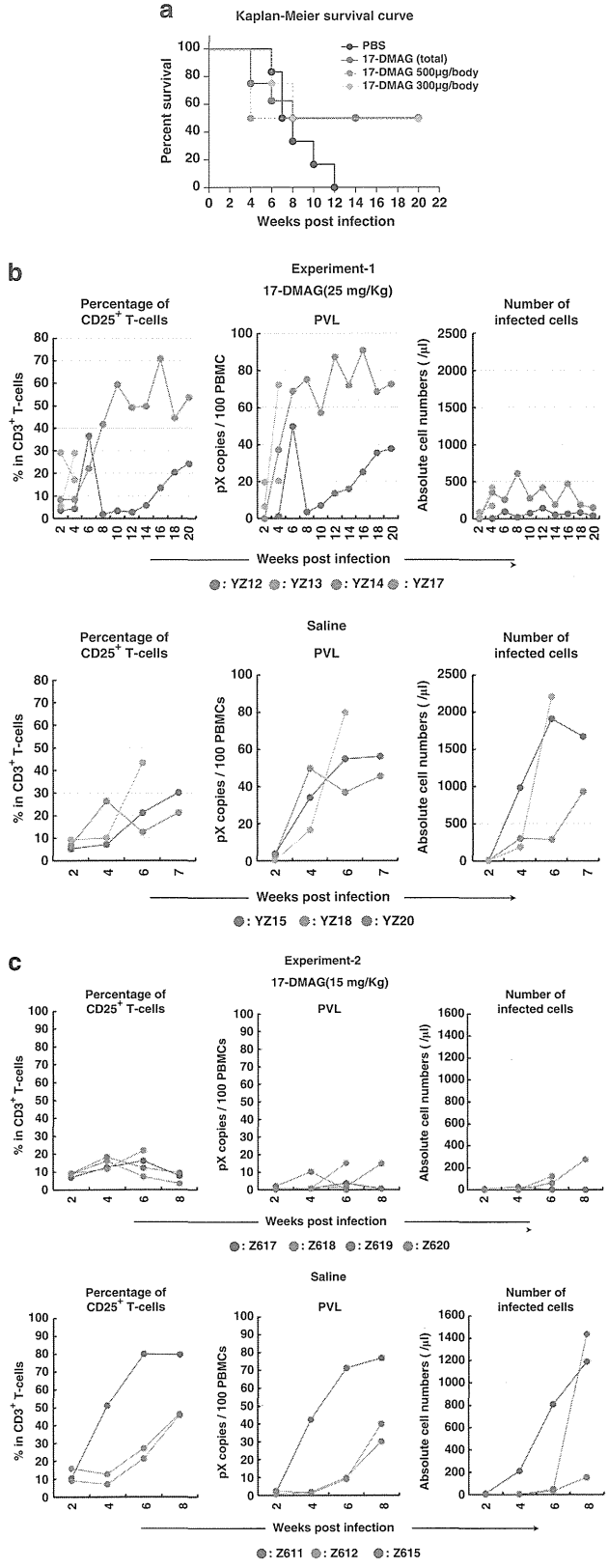

An oral administration of 17-DMAG to ATL model mice induced blockade of aggressive proliferation and multiple tissue invasions of transformed lymphocytes and improved survival rate

The demonstration that 17-DMAG has profound effects on Tax stability and the fact that it is water soluble suggested that this compound could be tested in a recently developed preclinical model of ATL.[23,28]

SCID mice were injected with 2×10^6 Lck-Tax cells intraperitoneally and treated for 5 consecutive days per week for 2 weeks with saline alone or with 17-DMAG in saline at 5 or 15 mg/kg. Mice were euthanized 21 days after cell inoculation. The blood smear indicated apparent reduction of Lck-Tax cells with increasing doses of 17-DMAG to saline controls (Figures 5a, e and i), although the quantitative cell counts were not obtained. The white pulp in greatly enlarged spleens (splenomegaly) of control mice was markedly expanded with red pulp compression (Figure 5b), and the livers and lungs of saline control mice were characterized by extensive perivascular infiltrations with Lck-Tax cells (Figures 5c and d). These pathologies were progressively reduced in mice treated with 17-DMAG (spleen, Figures 5f and j; liver, Figures 5g and k; and lung, Figures 5h and l).

We then determined the survival improvement through 17-DMAG oral administration with another preclinical ATL model (Figure 6). Each 7 (14 in total) huNOG mice[28] were injected with 1×10^6 HTLV-1-producing JEX cells (details are described in Supplementary Information), and 2 weeks after inoculation, each 4 of these mice (8 in total) were treated 20 times with 15 or 25 mg/kg of 17-DMAG for 4 weeks (as shown in Supplementary Figure 4), whereas the remaining 6 mice received saline only. The percentage of CD25-positive T cells, proviral load and the number of human leukocytes in peripheral blood were monitored. Four of eight 17-DMAG-treated mice died within 8 weeks post inoculation probably because of high drug dosage, but other four mice (50%) survived more than 20 weeks, whereas all the saline-treated controls died within 12 weeks post inoculation. The average survival period of controls and 17-DMAG-treated subjects were 8.33 and 14.75 weeks, respectively. However, the survival periods of 17-DMAG-treated subjects could be extended because four subjects were sacrificed at 24 weeks post inoculation for pathological examination (Supplementary Figure 4). The numbers of HTLV-1-infected human leukocytes in peripheral blood of 17-DMAG-treated subjects were also 5–10 times fewer than those of saline controls (Figures 6b and c).

Additive effects for growth arrest and apoptosis induction by concomitant 17-DMAG/Nutlin-3a treatment against ATL cells

The standard chemotherapy against ATL, named as leukemia study group 15 (LSG15), is currently employing the combination of four different anticancer drugs that frequently brings serious side effects to patients.[40] We previously demonstrated that a novel MDM-2-antagonizing/p53-stabilizing drug, Nutlin-3a, induces

Figure 6. Improved survival and suppression of the growth of HTLV-1-infected T cells by 17-DMAG oral treatment. (**a**) Kaplan–Meier survival curve of HTLV-1-infected huNOG mice. All mice have reconstituted human immune system by the transplantation of hematopoietic stem cells (huNOG) and have received 1 million JEX cells, which produce HTVL-1 infectious virus (see the details in Supplementary Figure 4). JEX/huNOG mice received 17-DMAG by oral administration for 4 weeks (2–6 weeks post inoculation, five times/week) at the dosage of 25 mg/kg (orange line) and 15 mg/kg (pink line). Control mice received the same volume of PBS. (**b**) The percentage of CD25-positive T cells, PVL and the number of HTLV-1-infected cells in peripheral blood of infected mice are shown. Upper panel represents the results from 17-DMAG-treated (25 mg/kg) mice; lower panel represents those of control mice. (**c**) Same experiments with 17-DMAG (15 mg/kg, upper panel) and PBS control (lower panel). PBS, phosphate buffered saline; PVL, proviral load.

the senescent death to ATL cells.[41] We then examined the additive anti-ATL effects of 17-DMAG and Nutlin-3a. Suboptimal dose of 17-DMAG (0.1 μM) or Nutlin-3a (1 μM) alone did not induce sufficient apoptotic or growth-arrest activities to ATL cell lines. However, the combined use of both induced significant growth suppressive and apoptotic properties (Figure 7), suggesting the possible combinational use of these drugs for further clinical studies.

DISCUSSION

HTLV-1 is the etiologic agent of ATL. Current studies indicate that worldwide there are more than 20 million HTLV-1 carriers and that 5% of these carriers will develop ATL.[42] The current standard for treatment of acute- or lymphoma-type ATL in Japan is CHOP or its modified regimen LSG15; however, the responses to this treatment regimen are limited to 31.1% of patients with 2-year survivals.[40] As malignant cells from relapsed patients are also resistant to other chemotherapeutic interventions, novel strategies for treatment of ATL are urgently required.

In this study, we demonstrated the significant inhibitory effects of 17-DMAG on Tax-mediated NF-κB signaling *in vitro* and *ex vivo*. The most striking observations obtained *in vitro* were (a) 17-DMAG-induced Tax degradation that resulted from inhibiting the formation of the Tax–IKK–HSP90/CDC37 ternary complex (Figures 1a–d); (b) induction of growth suppression and apoptosis of ATL cells while having little or no effect on normal PBLs (Figures 2a and b). We also found that the stability of Tax was heavily dependent on the CBD of CDC37 (Figures 4a and b). GA-dependent NF-κB downregulation in ATL cells was reported, and inhibition of autophagic activity seemed to affect the conversion of p100 (NF-κB2 precursor) to active p52.[32] We observed this time 17-DMAG-dependent Tax degradation and its blockade by AICAR and 3-MA (autophagy inhibitors) but not by the proteasome inhibitor MG-132 (Figure 1d), suggesting the direct involvement of the autophagosome on Tax metabolism in cells. This issue should further be investigated with ubiquitylation-deficient mutants Tax[24,31] or the autophagy-deficient cells.[43,44]

The CBD of CDC37 has been reported to bind preferentially to a specific glycine-rich motif — GXGXXG.[45] Indeed, Tax has a similar motif in its N terminus. CBD played crucial roles in stabilizing Tax and Tax–CDC37 complex formation (Figures 4c and d). CBD-containing mutants of CDC37 seemed to enhance the machinery responsible for Tax degradation as we did not detect any decrease in Tax levels in response to an siRNA knockdown of CDC37 (Supplementary Figure 5). Interestingly, the Tax-destabilizing CDC37(N200) translocated Tax to the nucleus, whereas wild-type CDC37 stayed with Tax in the cytoplasm (Figure 4d), and it implies that this translocation could be related to the Tax destabilization. For the future, it would be worth trying to identify a chemical compound that mimics the structure of CBD and could function as an inducer of Tax degradation. HSP90 and its co-chaperone's involvement in multiple signaling cascades, especially, in cancer cells, has been reported.[46,47] Indeed, 17-DMAG also suppressed NF-κB signaling mediated by other activators NIK, MEKK1, AKT, TAB2 and IKKα/β (data not shown). We also found that 17-DMAG treatment induced Tax degradation; potentially 17-DMAG treatment may also have led to the destabilization of other NF-κB signaling activators.

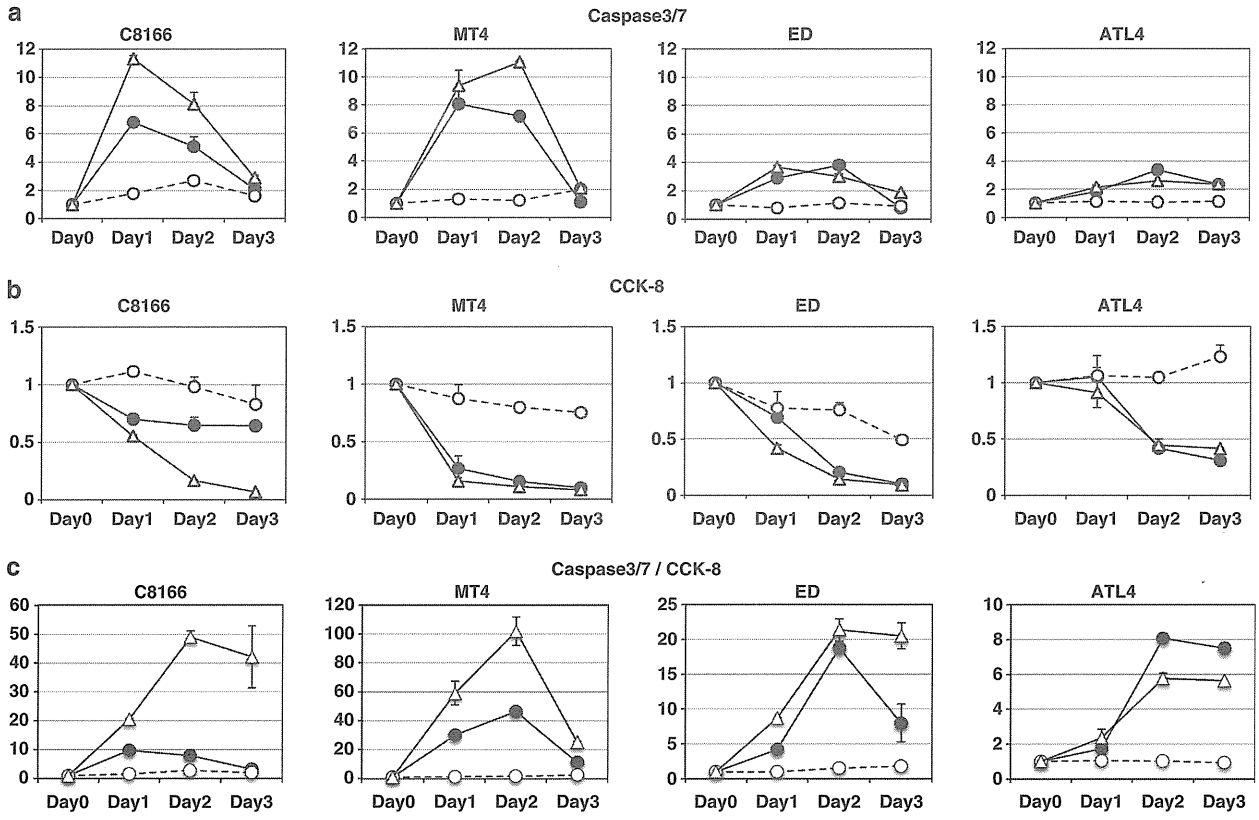

Figure 7. Additive anti-ATL cell effects by the combined dosage of 17-DMAG and Nutlin-3a. (**a**) ATL cell lines C8166, MT4, ED and ATL4 were treated with either suboptimal single dose of 17-DMAG (0.1 μM, black circles) and Nutlin-3a (1 μM, white circles)[41] or both (white triangles) for 3 days and harvested for caspase-3/7 assays (**a**) or CCK-8 assays (**b**) as described in Figure 2. Each untreated cell's value was set as 1. (**c**) Each caspase-3/7 (apoptotic) value was divided by CCK-8 (growth arrest) value to manifest the additive effects (see the Discussion section). CCK-8, Cell Counting Kit 8.

We have determined the therapeutic effects of 17-DMAG on two different ATL model systems through its oral administration. First, we tested 17-DMAG induced prevention of Lck-Tax infiltration in SCID mice, and 5 and 15 mg/kg of oral administration of 17-DMAG for 2 weeks reduced 74% and 83% of Lck-Tax cells, respectively; splenomegaly or massive infiltration of Lck-Tax cells into livers and lungs was also significantly reduced (Figure 5). In all experiments, 17-DMAG mice did not show any body weight losses or inactiveness compared with saline controls.

We then switched to another ATL model experiment JEX/huNOG, which has humanized immune environment in NOG mice and has inoculated HTLV-1-producing Jurkat cells. With oral administration of both 15 and 25 mg/kg 17-DMAG to JEX/huNOG, four of eight mice survived more than 20 weeks, whereas saline controls died within 12 weeks (Figure 6a). 17-DMAG treatment also reduced the number of HTLV-1-infected cells in peripheral blood, suggesting that 17-DMAG treatment could intervene the clonal T-cell development to ATL (Figure 6b). Although this preliminary experiment did not provide statistically significant survival rates, efficacy of this treatment is indeed highly expected. It is necessary to find the optimized conditions suppressing the ATL cell proliferation without any serious side effects.

Tax has pleiotropic effects on intra-cellular or inter-cellular signalings including mitotic checkpoint disruption,[48] aberrant cell-cycle progression[49,50] and altered chemotaxis.[51] The present ATL treatment protocols target the cytoskeletons or DNA replications with multiple doses of anticancer drugs (called as LSG15), and significant side effects by this treatment have been frequently recognized.[40] We have recently demonstrated the potential uses of molecularly targeted inhibitors of ATL cell proliferation, such as a MDM-2 ubiquitin ligase inhibitor Nutlin-3a[41] or CXCR4 antagonist AMD3100.[51] Nutlin-3a induces growth arrest and senescent-cell death of ATL cells at the 10 μM concentration, but normal PBLs are also significantly affected.[41] The combined use of 17-DMAG (0.1 μM) and Nutlin-3a (1 μM), suboptimal concentration for single use, significantly enhanced both apoptotic and growth suppressive effects (Figures 7a and b). This concurrent effects can be manifested with the division of caspase-3/7 values by Cell Counting Kit 8 values (Figure 7c). Besides Nutlin-3a, we also tested the efficacy of 17-DMAG plus LSG15 (without predonisolone; Supplementary Figure 6). Unlike the results of 17-DMAG/Nutlin-3a, 17-DMAG/LSG15 did not show any clear additive effects probably because LSG15 affects cell-cycle progression with a wide range of spectrum, but the effects of Nutlin-3a are specifically restricted to p53 stabilization.

It remains to be seen whether 17-DMAG is effective for ATL patients' treatment; elsewhere Hertlein *et al.*[52] have reported 17-DMAG's clinical application against chronic lymphocytic leukemia. Perhaps in future studies, 17-DMAG and other new drugs with novel anti-ATL activities such as Nutlin-3a, AMD3100 or a monoclonal anti-CCR4 antibody (KW-0761)[53] will provide more effective and less toxic ATL therapy.

CONFLICT OF INTEREST

The authors declare no conflict of interest.

ACKNOWLEDGEMENTS

We are indebted to Dr Herbert C Morse III for his helpful discussion and comments. We thank Mr T Kawashima and Ms Y Itoh for technical assistance and Drs K Terasawa, C Pique and K Nagata for providing plasmid DNAs. EI was a research fellow of the Okinawa Science and Technology Promotion Center. This study was supported in part by grants from the Ministry of Education, Culture, Sports, Science and Technology; the Ministry of Health, Labor and Welfare; the Ministry of Economy, Trade and Industry; Japan Science and Technology Agency; Okinawa Science and Technology Promotion Center; and Miyazaki Prefectural Industrial Support Foundation.

AUTHOR CONTRIBUTIONS

HI, J-IF and HdH designed the research; HdH, HS, WWH, KT, TU and J-IF developed the ATL animal model; EI, AK, KT, ST, SH, TMa, TU, TMi, KS, J-IF, HdH and HI performed the research; AN, MH, HrH, YY, YT, HS, WH, YM, KTJ, MO and KM contributed new reagents/materials; AK, KT, J-IF and HdH contributed pathologic analysis; and EI, KT, J-IF, HdH and HI wrote the paper.

REFERENCES

1 Li Q, Verma IM. NF-kappaB regulation in the immune system. *Nat Rev Immunol* 2002; **2**: 725–734.
2 Janssens S, Tschopp J. Signals from within: the DNA-damage-induced NF-kappaB response. *Cell Death Differ* 2006; **13**: 773–784.
3 Karin M. NF-kappaB as a critical link between inflammation and cancer. *Cold Spring Harb Perspect Biol* 2009; **1**: a000141.
4 Hayden MS, Ghosh S. Shared principles in NF-kappaB signaling. *Cell* 2008; **132**: 344–362.
5 Li XH, Fang X, Gaynor RB. Role of IKK-gamma/NEMO in assembly of the I-kappaB kinase complex. *J Biol Chem* 2001; **276**: 4494–4500.
6 Li Q, Van Antwerp D, Mercurio F, Lee KF, Verma IM. Severe liver degeneration in mice lacking the I-kappaB kinase 2 gene. *Science* 1999; **284**: 321–325.
7 Schmidt-Supprian M, Bloch W, Courtois G, Addicks K, Israel A, Rajewsky K *et al.* NEMO/IKK-gamma-deficient mice model incontinentia pigmenti. *Mol Cell* 2000; **5**: 981–992.
8 Li Q, Lu Q, Hwang JY, Buscher D, Lee KF, Izpisua-Belmonte JC *et al.* IKK1-deficient mice exhibit abnormal development of skin and skeleton. *Genes Dev* 1999; **13**: 1322–1328.
9 Takeda K, Takeuchi O, Tsujimura T, Itami S, Adachi O, Kawai T *et al.* Limb and skin abnormalities in mice lacking IKK-alpha. *Science* 1999; **284**: 313–316.
10 Yamaoka S, Courtois G, Bessia C, Whiteside ST, Weil R, Agou F *et al.* Complementation cloning of NEMO, a component of the I-kappaB kinase complex essential for NF-kappaB activation. *Cell* 1998; **93**: 1231–1240.
11 Iha H, Kibler KV, Yedavalli VR, Peloponese JM, Haller K, Miyazato A *et al.* Segregation of NF-kappaB activation through NEMO/IKK-gamma by Tax and TNF-alpha: implications for stimulus-specific interruption of oncogenic signaling. *Oncogene* 2003; **22**: 8912–8923.
12 Chen G, Cao P, Goeddel DV. TNF-induced recruitment and activation of the IKK complex require Cdc37 and Hsp90. *Mol Cell* 2002; **9**: 401–410.
13 Bouwmeester T, Bauch A, Ruffner H, Angrand PO, Bergamini G, Croughton K *et al.* A physical and functional map of the human TNF-alpha/NF-kappa B signal transduction pathway. *Nat Cell Biol* 2004; **6**: 97–105.
14 Yoshida M. Multiple viral strategies of HTLV-1 for dysregulation of cell growth control. *Annu Rev Immunol* 2001; **19**: 475–496.
15 Hall WW, Fujii M. Deregulation of cell-signaling pathways in HTLV-1 infection. *Oncogene* 2005; **24**: 5965–5975.
16 Matsuoka M, Jeang KT. Human T-cell leukaemia virus type 1 (HTLV-1) infectivity and cellular transformation. *Nat Rev Cancer* 2007; **7**: 270–280.
17 Jin DY, Giordano V, Kibler KV, Nakano H, Jeang KT. Role of adapter function in oncoprotein-mediated activation of NF-kappaB. Human T-cell leukemia virus type I Tax interacts directly with I-kappaB kinase gamma. *J Biol Chem* 1999; **274**: 17402–17405.
18 Carter RS, Pennington KN, Ungurait BJ, Ballard DW. *In vivo* identification of inducible phosphoacceptors in the IKK-gamma/NEMO subunit of human I-kappaB kinase. *J Biol Chem* 2003; **278**: 19642–19648.
19 Lamsoul I, Lodewick J, Lebrun S, Brasseur R, Burny A, Gaynor RB *et al.* Exclusive ubiquitination and sumoylation on overlapping lysine residues mediate NF-kappaB activation by the human T-cell leukemia virus Tax oncoprotein. *Mol Cell Biol* 2005; **25**: 10391–10406.
20 Chu ZL, DiDonato JA, Hawiger J, Ballard DW. The Tax oncoprotein of human T-cell leukemia virus type 1 associates with and persistently activates I-kappaB kinases containing IKK-alpha and IKK-beta. *J Biol Chem* 1998; **273**: 15891–15894.
21 Geleziunas R, Ferrell S, Lin X, Mu Y, Cunningham Jr ET, Grant M *et al.* Human T-cell leukemia virus type 1 Tax induction of NF-kappaB involves activation of the I-kappaB kinase alpha (IKK-alpha) and IKK-beta cellular kinases. *Mol Cell Biol* 1998; **18**: 5157–5165.
22 Egorin MJ, Lagattuta TF, Hamburger DR, Covey JM, White KD, Musser SM *et al.* Pharmacokinetics, tissue distribution, and metabolism of 17-(dimethylaminoethylamino)-17-demethoxygeldanamycin (NSC 707545) in CD2F1 mice and Fischer 344 rats. *Cancer Chemother Pharmacol* 2002; **49**: 7–19.
23 Hasegawa H, Sawa H, Lewis MJ, Orba Y, Sheehy N, Yamamoto Y *et al.* Thymus-derived leukemia–lymphoma in mice transgenic for the Tax gene of human T-lymphotropic virus type I. *Nat Med* 2006; **12**: 466–472.

24 Chiari E, Lamsoul I, Lodewick J, Chopin C, Bex F, Pique C. Stable ubiquitination of human T-cell leukemia virus type 1 tax is required for proteasome binding. *J Virol* 2004; **78**: 11823–11832.
25 Momose F, Naito T, Yano K, Sugimoto S, Morikawa Y, Nagata K. Identification of Hsp90 as a stimulatory host factor involved in influenza virus RNA synthesis. *J Biol Chem* 2002; **277**: 45306–45314.
26 Terasawa K, Minami Y. A client-binding site of Cdc37. *FEBS J* 2005; **272**: 4684–4690.
27 Ueyama T, Kusakabe T, Karasawa S, Kawasaki T, Shimizu A, Son J *et al.* Sequential binding of cytosolic Phox complex to phagosomes through regulated adaptor proteins: evaluation using the novel monomeric Kusabira-Green system and live imaging of phagocytosis. *J Immunol* 2008; **181**: 629–640.
28 Nie C, Sato K, Misawa N, Kitayama H, Fujino H, Hiramatsu H *et al.* Selective infection of CD4+ effector memory T lymphocytes leads to preferential depletion of memory T lymphocytes in R5 HIV-1-infected humanized NOD/SCID/IL-2Rgammanull mice. *Virology* 2009; **394**: 64–72.
29 Ueno S, Umeki K, Takajo I, Nagatomo Y, Kusumoto N, Umekita K *et al.* Proviral loads of human T-lymphotropic virus type 1 in asymptomatic carriers with different infection routes. *Int J Cancer* 2012; **130**: 2318–2326.
30 De Valck D, Jin DY, Heyninck K, Van de Craen M, Contreras R, Fiers W *et al.* The zinc finger protein A20 interacts with a novel anti-apoptotic protein which is cleaved by specific caspases. *Oncogene* 1999; **18**: 4182–4190.
31 Peloponese JM, Iha H, Yedavalli VR, Miyazato A, Li Y, Haller K *et al.* Ubiquitination of human T-cell leukemia virus type 1 tax modulates its activity. *J Virol* 2005; **78**: 11686–11695.
32 Yan P, Qing G, Qu Z, Wu CC, Rabson A, Xiao G. Targeting autophagic regulation of NFkappaB in HTLV-I transformed cells by geldanamycin: implications for therapeutic interventions. *Autophagy* 2007; **3**: 600–603.
33 Mitsiades CS, Mitsiades NS, McMullan CJ, Poulaki V, Kung AL, Davies FE *et al.* Antimyeloma activity of heat shock protein-90 inhibition. *Blood* 2006; **107**: 1092–1100.
34 Jeang KT, Chiu R, Santos E, Kim SJ. Induction of the HTLV-I LTR by Jun occurs through the Tax-responsive 21-bp elements. *Virology* 1991; **181**: 218–227.
35 Prodromou C, Roe SM, O'Brien R, Ladbury JE, Piper PW, Pearl LH. Identification and structural characterization of the ATP/ADP-binding site in the Hsp90 molecular chaperone. *Cell* 1997; **90**: 65–75.
36 Meyer P, Prodromou C, Hu B, Vaughan C, Roe SM, Panaretou B *et al.* Structural and functional analysis of the middle segment of hsp90: implications for ATP hydrolysis and client protein and cochaperone interactions. *Mol Cell* 2003; **11**: 647–658.
37 Minami Y, Kimura Y, Kawasaki H, Suzuki K, Yahara I. The carboxy-terminal region of mammalian HSP90 is required for its dimerization and function *in vivo*. *Mol Cell Biol* 1994; **14**: 1459–1464.
38 Roe SM, Ali MM, Meyer P, Vaughan CK, Panaretou B, Piper PW *et al.* The mechanism of Hsp90 regulation by the protein kinase-specific cochaperone p50(cdc37). *Cell* 2004; **116**: 87–98.
39 Silverstein AM, Grammatikakis N, Cochran BH, Chinkers M, Pratt WB. p50(cdc37) binds directly to the catalytic domain of Raf as well as to a site on hsp90 that is topologically adjacent to the tetratricopeptide repeat binding site. *J Biol Chem* 1998; **273**: 20090–20095.
40 Uozumi K. Treatment of adult T-cell leukemia. *J Clin Exp Hematop* 2010; **50**: 9–25.
41 Hasegawa H, Yamada Y, Iha H, Tsukasaki K, Nagai K, Atogami S *et al.* Activation of p53 by Nutlin-3a, an antagonist of MDM2, induces apoptosis and cellular senescence in adult T-cell leukemia cells. *Leukemia* 2009; **23**: 2090–2101.
42 Proietti FA, Carneiro-Proietti AB, Catalan-Soares BC, Murphy EL. Global epidemiology of HTLV-I infection and associated diseases. *Oncogene* 2005; **24**: 6058–6068.
43 Mizushima N, Yoshimori T, Ohsumi Y. The role of Atg proteins in autophagosome formation. *Annu Rev Cell Dev Biol* 2011; **27**: 107–132.
44 Codogno P, Mehrpour M, Proikas-Cezanne T. Canonical and non-canonical autophagy: variations on a common theme of self-eating? *Nat Rev Mol Cell Biol* 2011; **13**: 7–12.
45 Terasawa K, Yoshimatsu K, Iemura SI, Natsume T, Tanaka K, Minami Y. Cdc37 interacts with the glycine-rich loop of Hsp90 client kinases. *Mol Cell Biol* 2006; **26**: 3378–3389.
46 Calderwood SK, Khaleque MA, Sawyer DB, Ciocca DR. Heat shock proteins in cancer: chaperones of tumorigenesis. *Trends Biochem Sci* 2006; **31**: 164–172.
47 Caplan AJ, Mandal AK, Theodoraki MA. Molecular chaperones and protein kinase quality control. *Trends Cell Biol* 2007; **17**: 87–92.
48 Jin DY, Spencer F, Jeang KT. Human T cell leukemia virus type 1 oncoprotein Tax targets the human mitotic checkpoint protein MAD1. *Cell* 1998; **93**: 81–91.
49 Giam CZ, Jeang KT. HTLV-1 Tax and adult T-cell leukemia. *Front Biosci* 2007; **12**: 1496–1507.
50 Tanaka Y. Activation of leukocyte function-associated antigen-1 on adult T-cell leukemia cells. *Leuk Lymphoma* 1999; **36**: 15–23.
51 Kawaguchi A, Orba Y, Kimura T, Iha H, Ogata M, Tsuji T *et al.* Inhibition of the SDF-1alpha-CXCR4 axis by the CXCR4 antagonist AMD3100 suppresses the migration of cultured cells from ATL patients and murine lymphoblastoid cells from HTLV-I Tax transgenic mice. *Blood* 2009; **114**: 2961–2968.
52 Hertlein E, Wagner AJ, Jones J, Lin TS, Maddocks KJ, Towns III WH *et al.* 17-DMAG targets the nuclear factor-kappaB family of proteins to induce apoptosis in chronic lymphocytic leukemia: clinical implications of HSP90 inhibition. *Blood* 2010; **116**: 45–53.
53 Yamamoto K, Utsunomiya A, Tobinai K, Tsukasaki K, Uike N, Uozumi K *et al.* Phase I study of KW-0761, a defucosylated humanized anti-CCR4 antibody, in relapsed patients with adult T-cell leukemia–lymphoma and peripheral T-cell lymphoma. *J Clin Oncol* 2010; **28**: 1591–1598.

Supplementary Information accompanies this paper on the Blood Cancer Journal website (http://www.nature.com/bcj).

Virology 443 (2013) 226–235

Contents lists available at SciVerse ScienceDirect

Virology

journal homepage: www.elsevier.com/locate/yviro

Failure in activation of the canonical NF-κB pathway by human T-cell leukemia virus type 1 Tax in non-hematopoietic cell lines

Terumi Mizukoshi [a], Hideyuki Komori [a,1], Mariko Mizuguchi [a], Hussein Abdelaziz [a,b], Toshifumi Hara [a,2], Masaya Higuchi [c], Yuetsu Tanaka [d], Yoshiro Ohara [e], Noriko Funato [a], Masahiro Fujii [c], Masataka Nakamura [a,*]

[a] Human Gene Sciences Center, Tokyo Medical and Dental University, 1-5-45 Yushima, Bunkyo-ku, Tokyo 113-8510, Japan
[b] Department of Medical Biochemistry, Faculty of Medicine, Mansoura University, Mansoura, Egypt
[c] Division of Virology, Niigata University Graduate School of Medical and Dental Sciences, Niigata, Japan
[d] Department of Immunology, Graduate School and Faculty of Medicine, Ryukyu University, Okinawa, Japan
[e] Department of Microbiology, Kanazawa Medical University, Ishikawa, Japan

ARTICLE INFO

Article history:
Received 21 January 2013
Returned to author for revisions
25 February 2013
Accepted 29 April 2013
Available online 18 June 2013

Keywords:
HTLV-1
Tax1
NF-κB
Canonical pathway
Transcription
Hematopoietic cells

ABSTRACT

Human T-cell leukemia virus type 1 (HTLV-1) Tax (Tax1) plays crucial roles in leukemogenesis in part through activation of NF-κB. In this study, we demonstrated that Tax1 activated an NF-κB binding (gpκB) site of the gp34/OX40 ligand gene in a cell type-dependent manner. Our examination showed that the gpκB site and authentic NF-κB (IgκB) site were activated by Tax1 in hematopoietic cell lines. Non-hematopoietic cell lines including hepatoma and fibroblast cell lines were not permissive to Tax1-mediated activation of the gpκB site, while the IgκB site was activated in those cells in association with binding of RelB. However RelA binding was not observed in the gpκB and IgκB sites. Our results suggest that HTLV-1 Tax1 fails to activate the canonical pathway of NF-κB in non-hematopoietic cell lines. Cell type-dependent activation of NF-κB by Tax1 could be associated with pathogenesis by HTLV-1 infection.

Introduction

Infection with human T-cell leukemia virus type1 (HTLV-1) causes adult T-cell leukemia (ATL) and inflammatory disorders such as HTLV-1 associated myelopathy/tropical spastic paraparesis and HTLV-1 associated uveitis (Hinuma et al., 1981; Osame et al., 1986; Poiesz et al., 1980). HTLV-1 encodes Tax1, which has been shown to be implicated in the pathogenesis of HTLV-1 associated disorders (Giam and Jeang, 2007). Tax1 is a trans-acting transcriptional regulator that exerts its function via cellular transcription factors mainly cAMP responsive element binding protein (CREB), nuclear factor κB (NF-κB) and serum responsive factor (SRF) (Ballard et al., 1988; Fujii et al., 1992; Lenzmeier et al., 1998). Tax1 interaction with cellular transcription factors leads to transcriptional changes in many cellular genes as well as activation of HTLV-1 transcription (Lenzmeier et al., 1998; Ohtani and Nakamura, 2002; Yoshida M., 2001; Zhao and Giam, 1992). Previous studies demonstrated that activation of NF-κB by Tax1 is closely associated with development and maintenance of ATL (Akagi et al., 1995; Ben-Neriah and Karin, 2011; Matsuoka and Jeang, 2007; Qu and Xiao, 2011). Tax1 activates both the NF-κB canonical and non-canonical pathways consisting of RelA with p50 and RelB with p52, respectively (Harhaj and Harhaj, 2005; Xiao et al., 2001). Activation of the canonical pathway results mainly from association of Tax1 with the IKK complex, leading to inactivation of IκB by phosphorylation, followed by translocation of the RelA/p50 complex to the nucleus (Geleziunas et al., 1998; Jin et al., 1999). Tax1 is also able to directly facilitate the transition of the precursor p100 into p52, thus promoting translocation of the non-canonical pathway complex RelB with p52 to the nucleus (Higuchi et al., 2007; Shoji et al., 2009). In the nucleus, NF-κB binds promoter DNA elements to initiate or enhance transcription of respective genes. The other member of the HTLV family is HTLV-2, which also produces a trans-acting transcriptional molecule so-called Tax2 (Ross et al., 1996). Tax2 does resemble Tax1 in terms of the ability to activate NF-κB and differs from Tax1 in that Tax2 predominantly activates the canonical NF-κB pathway (Higuchi et al., 2007; Shoji et al., 2009).

The gp34 gene was first identified to be a target of Tax1 in human T cells (Miura et al., 1991; Tanaka et al., 1985). Since its discovery, the gene product has been revealed as an OX40 ligand (OX40L), a type II transmembrane member of the tumor necrosis factor (TNF) superfamily, which is expressed on antigen presenting

* Corresponding author. Fax: +81 3 5803 0234.
E-mail address: naka.gene@tmd.ac.jp (M. Nakamura).
[1] Present address: Life Science Institute, University of Michigan, Ann Arbor, MI, USA.
[2] Present address: Genetics Branch, National Cancer Institute, National Institutes of Health, Bethesda, MD, USA.

0042-6822/$ - see front matter © 2013 Elsevier Inc. All rights reserved.
http://dx.doi.org/10.1016/j.virol.2013.04.032

cells, endothelial cells and activated T cells under normal immune conditions (Baum et al., 1994). OX40L interacts with OX40, a member of the TNF receptor family, which is predominantly expressed in T cell and delivers co-stimulatory signals implicated in expansion, survival and homeostasis of T cells (Ishii et al., 2010). Among ATL cells and HTLV-1 infected T cells, only T cells expressing Tax1 express OX40L on their cell surface. We previously reported that the gp34 (OX40L) gene promoter has an element capable of NF-κB binding (Ohtani et al., 1998). The NF-κB binding (gpκB) site is, at least in part, responsible for Tax1-mediated expression of OX40L on T cells. This Tax1-mediated expression makes the interaction of OX40 with OX40L possible in the same T cells. OX40 and OX40L interaction in ATL development remains to be examined. Our preliminary results indicate that the gpκB site in the OX40L promoter is somewhat different from the classical NF-κB binding site represented by the NF-κB binding site (IgκB site) of the immunoglobulin light chain gene promoter. The gpκB site in the OX40L promoter fails to be activated in the presence of Tax1 in the fibroblast cell line REF52, in contrast to activation in the T cell line Jurkat.

In this study, we wished to understand how Tax1 activated the gpκB site in a cell type-dependent manner. Our results indicate that Tax1 does not activate the canonical NF-κB pathway in non-hematopoietic cell lines, suggesting involvement of Tax1 in T cell pathogenesis.

Results

Tax1 does not activate the gpκB site in non-hematopoietic cells

Tax1 activated the IgκB and gpκB sites in Jurkat cells (Fig. 1), as shown previously (Ohtani et al., 1998). Unexpectedly, in REF52 cells, Tax1 did not activate the gpκB site, while the IgκB site was activated (Fig. 1). We hypothesized that responses of the gpκB site to Tax1 might be cell lineage-dependent. To test this notion, more cell lines of hematopoietic and non-hematopoietic lineages were used for reporter assays with Tax1. Non-hematopoietic cell lines, the human osteosarcoma cell line MG63, the human hepatoma cell lines Huh7 and HepG2, the human cervical cancer cell line HeLa, the human embryonic kidney cell line 293T and the murine neuroblastoma cell line C-1300 exhibited Tax1-mediated activation of the IgκB site, but the gpκB site was not activated in response to Tax1 in those cell lines (Fig. 1). A slight but not significant activation of the gpκB site by Tax1 was observed in HeLa and 293T cells, however this activation may be due to indirect effects of Tax1 (discussed later). Hematopoietic cell lines, the human Burkitt's lymphoma cell line Raji and the human myelogenous leukemia cell line K562, allowed activation of the gpκB site by Tax1 similar to Jurkat (Fig. 1). These results suggest that Tax1 does not activate the gpκB site in non-hematopoietic lineage cell lines.

In order to study cell type-dependent activation of the gpκB site by Tax1, we examined effects of ectopic expression of NF-κB subunits (RelA, p105/p50, RelB, p100/p52 and c-Rel) on the activation of the gpκB site in non-hematopoietic cell lines. The gpκB site was activated by overexpression of either RelA or p50 without Tax1 in REF52, MG63 and HeLa cells (Fig. 2A). Similarly RelA-dependent activation was seen with the IgκB site (Fig. 2A). Increased activation by RelA was dose-dependent (Fig. S1). Ectopic expression of c-Rel slightly activated the gpκB site (Fig. 2A). Introduction of RelB or p52 combination however did not change reporter gene expression from the gpκB site, while the IgκB site was activated by treatment with RelB (Fig. 2A and B). These results suggest that the canonical pathway is closely associated with activation of the gpκB sites in non-hematopoietic cells.

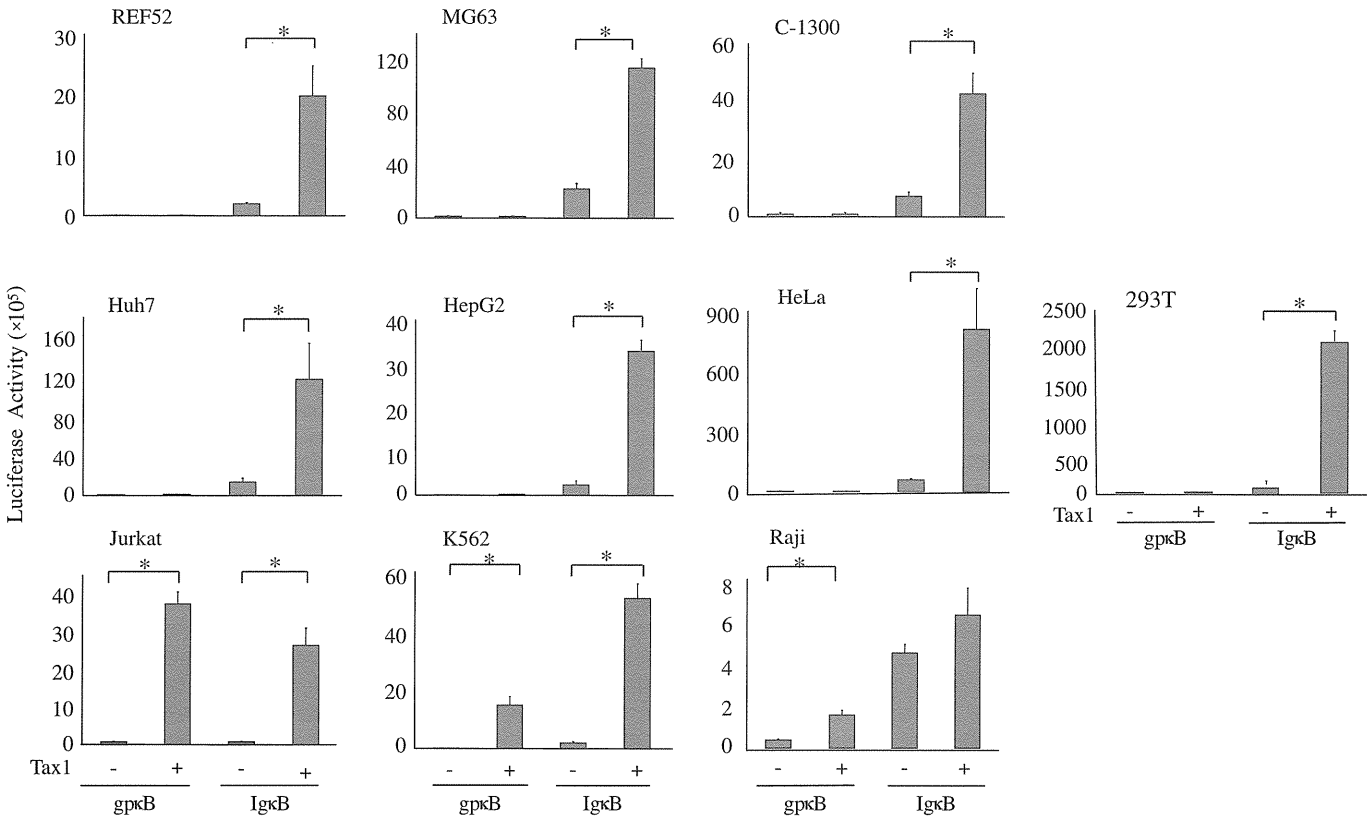

Fig. 1. Cell type-dependent activation of the gpκB site by Tax1. Cells were transfected with the gpκB or IgκB reporter plasmid along with pMT-2Tax. REF52, MG63, HeLa, 293T, Jurkat, K562 and Raji cells were cultured for 48 h. Huh7, HepG2 and C-1300 cells were cultured for 24 h and harvested for luciferase activity determination. Luciferase activity was normalized to protein content. Data are means ± SE. *$P < 0.05$.

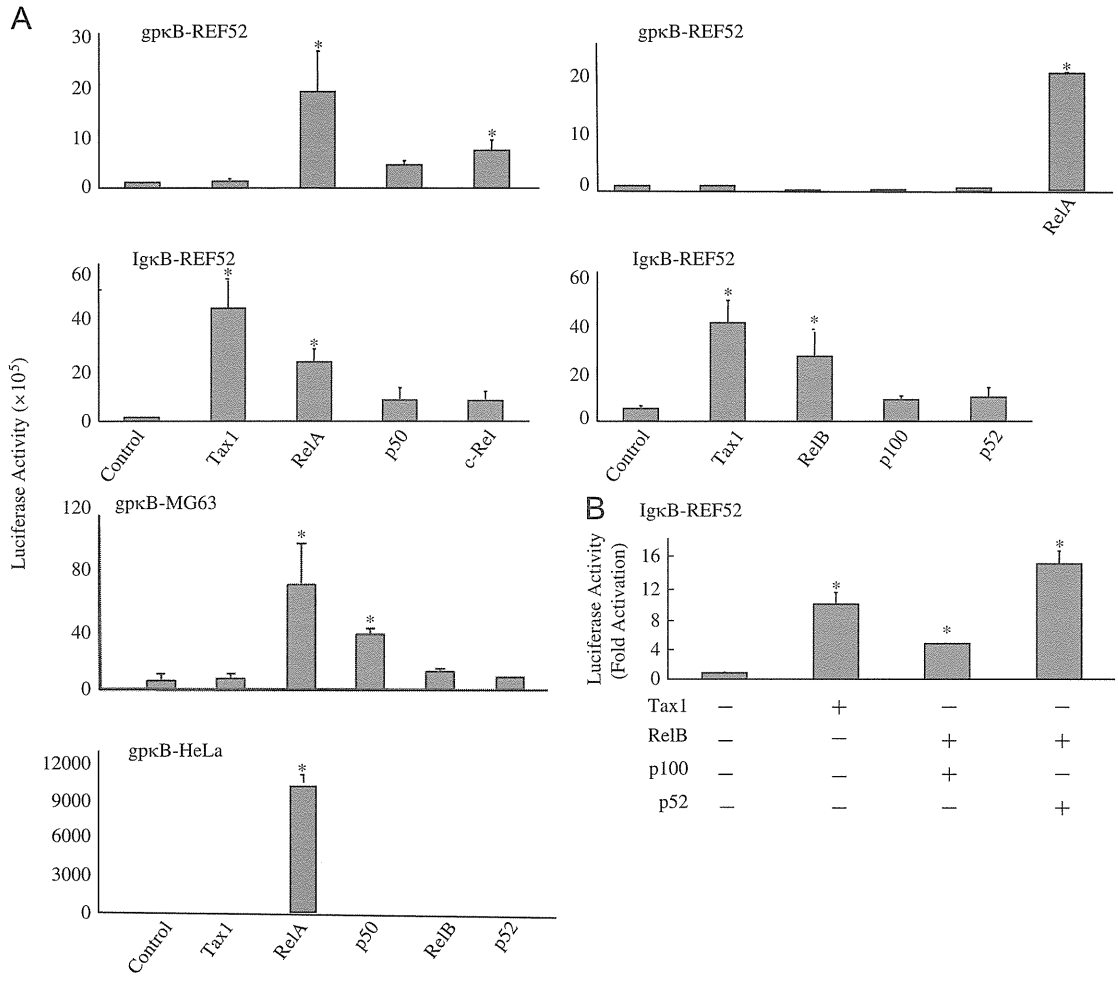

Fig. 2. Effects of NF-κB subunits on gpκB site activation. Expression plasmids for NF-κB subunits or Tax1 were transfected to REF52, HeLa and 293T cells along with the gpκB or IgκB reporter plasmid. Cells were cultured for 48 h and harvested for luciferase activity determination. Luciferase activity was normalized to protein content (A) or to β-galactosidase activity (B). Data are means ± SE. $^{*}P < 0.05$.

Tax1 activates the non-canonical NF-κB pathway in REF52 cells

Based on these results, we assumed the possibility that Tax1 did not activate the canonical pathway in non-hematopoietic cell lines and that the non-canonical pathway might be responsible for Tax1-dependent activation of the IgκB site. The assumption was examined by experiments with REF52 cells overexpressing the NF-κB subunits. Interestingly, overexpression of the non-canonical pathway subunit RelB alone or along with p52, a partner in the non-canonical pathway, significantly activated the IgκB sites in REF52 cells in the absence of Tax1 (Fig. 2A and B). Consistent with this, disruption of RelB or p52 by introduction of respective siRNA significantly reduced activation of the IgκB site by Tax1, while siRNA for RelA or p50 did not show appreciable effect (Fig. 3).

HTLV-2, a human retrovirus close to HTLV-1, produces Tax2, which is known to predominantly activate the canonical NF-κB pathway (Matsumoto et al., 1997). Similar to Tax1, Tax2 activated both gpκB and IgκB sites in Jurkat cells, while, in REF52 cells, the gpκB site was not activated by Tax2 (Fig. 4A). Tax2 exhibited significantly lower activation of the IgκB sites than Tax1 in REF52 cells (Fig. 4B). A chimera Tax mutant (Tax1/2) between Tax1 and Tax2, in which the Tax1 (225–232) region responsible for activation of the non-canonical pathway was replaced with a region of Tax2 (225–232), has little ability to activate the non-canonical pathway (Shoji et al., 2009). The effects of the Tax1/2 mutant on activation of the gpκB and IgκB sites were close to those of Tax2, rather than Tax1, in Jurkat and REF52 cells (Fig. 4). These results strongly indicate the possibilities that the gpκB site is activated by the canonical, but not non-canonical, pathway and that the canonical pathway is scarcely activated by Tax1 in non-hematopoietic cell lines.

RelA and p50 are expressed in non-hematoietic cells

We therefore examined expression and localization of NF-κB subunits in non-hematopoietic cells. Immunostaining and Western blot analyses clearly showed that REF52, MG63 and HeLa cells expressed RelA, p50, RelB and p52 (Fig. 5A–H). RelA was mainly present in the cytoplasm, while p50 was in the nucleus and cytoplasm (Fig. 5A–D). The ability of those subunits to bind κB sites was examined by electrophoreitic mobility shift assay (EMSA). In contrast to the cytoplasmic extracts which gave supershift bands with anti-RelA antibody, nuclear extracts from REF52 cells with or without Tax1 expression did not form complexes containing RelA with the gpκB site and the IgκB site (Fig. 6A and B). Binding of p50 was seen with both nuclear and cytoplasmic extracts; nuclear extracts from Tax1-expressing REF52 cells formed the most abundant complex. Ectopic expression of RelA in REF52 cells induced its complex formation with the gpκB site (Fig. 6C). Complexes containing RelA were also detected using nuclear extracts from REF52 cells ectopically expressing p50. These results are consistent with reporter assays. RelB, p52 and c-Rel were not included in complexes

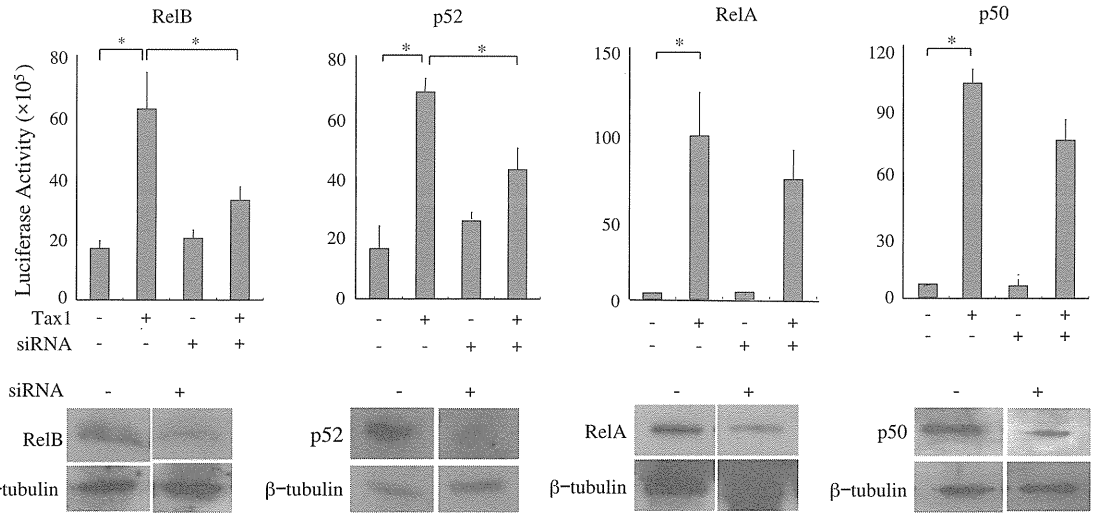

Fig. 3. Effects of siRNA for RelB, p52, RelA and p50 on κB site activation. REF52 cells were transfected with siRNA (10 nM) for RelB, p52, RelA and p50, and, one day after, introduced with pIgκB-Luc with or without pMT-2Tax in Lipofectamine 2000. Cells were harvested for luciferase activity determination 24 h after transfection with the reporter plasmid. Luciferase activity was normalized to protein content. Data are means ± SE. $^{*}P < 0.05$. Western blotting with antibodies to RelB, p52, RelA, p50 and β-tubulin was performed with lysates from cells transfected with siRNA.

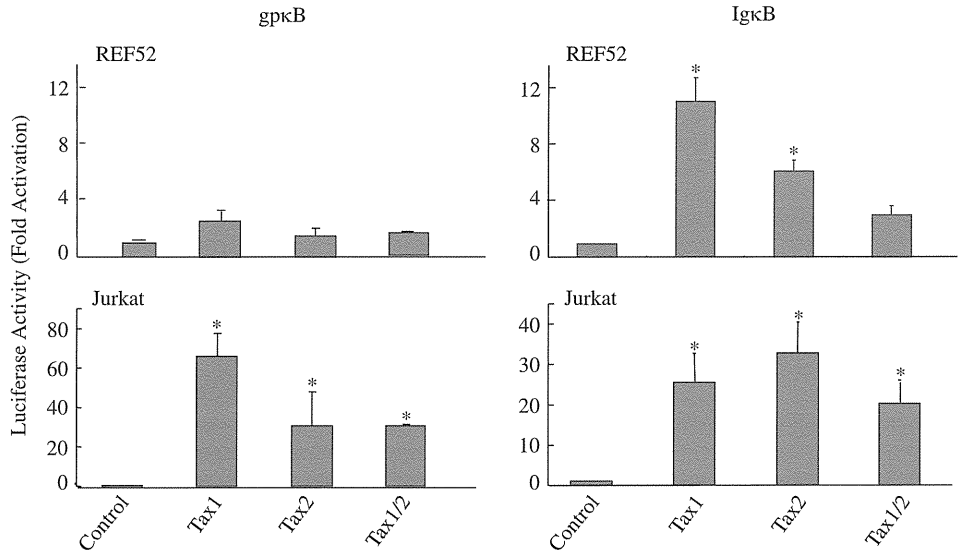

Fig. 4. Effects of Tax2 on gpκB site activation. REF52 and Jurkat cells were transfected with Tax1, Tax2 or Tax1/2 expression plasmid along with the gpκB or IgκB reporter plasmid and pCMV-β-gal. Cells were cultured for 48 h and harvested for luciferase activity determination. Luciferase activity was normalized to β-galactosidase activity. Data are means ± SE. $^{*}P < 0.05$.

formed with the gpκB site when nuclear extracts were prepared from Tax1-expressing REF52 cells (Fig. S2).

Immunofluorescence staining confirmed the results of EMSA. Tax1 introduction did not appreciably alter localization of RelA predominantly localized in the cytoplasm in those cells except for HeLa cells (Fig. 5A, C and D). In HeLa cells after Tax1 transfection, RelA was seen in the nucleus as well as the cytoplasm irrespective of Tax1 expression. This RelA expression might be attributable to Tax1-dependent paracrine mechanism, because HeLa cells even without Tax1 expression expressed RelA in the nucleus as indicated by arrowheads in Fig. 5D. The p50 molecule was mainly seen in the peri-nuclear region. RelB was present in the cytoplasm before introduction of Tax1 like RelA. In contrast to RelA, Tax1 facilitated the influx of RelB to the nucleus. Immunostaining with anti-p52 antibody detected p100/p52 mainly in the cytoplasm without Tax1 and in both the cytoplasm and nucleus with Tax1. Western blot examination also showed that RelB and p52 were seen in the nucleus after Tax1 was expressed, while RelA stayed in the cytoplasm even after Tax1 introduction in REF52 and MG63 cells (Fig. 5E and G). HeLa cells showed RelA translocation to the nucleus, as discussed before (Fig. 5H). In contrast, Jurkat cells exhibited translocation of RelA, as well as RelB and p52, in a Tax1-dependent manner (Fig. 5B and F).

RelA and p50 expressed in REF52 cells were examined for their function by stimulation with tumor necrosis factor α (TNFα). TNFα induced activation of the IgκB site in the luciferase reporter assays in association with translocation of RelA from the cytoplasm to the nucleus and phosphorylation of IκBα potentially leading to degradation (Fig. 5I–K). MG63 and HeLa cells also showed TNFα-induced RelA translocation (Fig. 5G and H). These

results suggest that RelA/p50 is functional in those non-hematopoietic cell lines.

Tax1 induces RelB and p52 binding to the IgκB site in vivo

In order to examine the ability of the IgκB site to bind NF-κB subunits in cells, we performed the chromatin immunoprecipitation (ChIP) assays in REF52, MG63 and HeLa cells with or without Tax1 expression (Fig. 7A, C and D). After reporter plasmid transfection with or without the Tax1 expression plasmid, cells were lysed and immunoprecipitated by anti-NF-κB subunit antibodies. None of the antibodies used precipitated appreciable gpκB and IgκB site DNA elements without Tax1 expression (Fig. 7A). Immunoprecipitation with anti-RelB, anti-p52 and anti-p50 antibodies detected the IgκB site with Tax1 expression. In addition, HeLa cells showed RelA binding to the IgκB site (Fig. 7D). As expected, only anti-p50 antibody precipitated the gpκB site in REF52 cells with Tax1 expression. Antibodies to RelA, RelB and p52 did not effectively precipitate the gpκB site in REF52 cells. These results indicate that at least REF52 and MG63 cells do not have the active form of the RelA/p50 complex in the nucleus in the presence of Tax1. In Jurkat cells, both the gpκB and IgκB sites were immunoprecipitated with all antibodies used in a Tax1-dependent manner (Fig. 7B).

Discussion

The present study demonstrates that the gpκB site is activated by HTLV-1 Tax1 in a cell type-dependent manner. Hematopoietic cell lines Jurkat, Raji and K562 activated the gpκB site upon Tax1 expression, whereas the seven non-hematopoietic cell lines failed to activate the gpκB site. One the other hand, the IgκB site was activated by Tax1 in both hematopoietic and non-hematopoietic cell lines used in this study. As overexpression of the canonical pathway subunit RelA activated the gpκB in non-hematopoietic cells, the gpκB unresponsiveness is presumably due to inactivation of the NF-κB canonical pathway by Tax1 in those cell lines. These results also suggest that the gpκB site is probably activated by the canonical pathway, but not by the non-canonical pathway, in the non-hematopoietic cell lines. Many NF-κB binding sites have been identified, most of which are activated by the canonical and non-canonical pathways. The gpκB site may be a unique case of NF-κB responsive elements that may discriminate the canonical pathway from the non-canonical pathway. Among three transcription factor pathways, involving NF-κB, CREB and SRF, which are directly activated by Tax1, Tax1-mediated NF-κB activation has been studied extensively and intensively. This is because ATL cells, including their derivative cell lines, carry constitutively active NF-κB (Yoshida et al., 1982). Studies suggest a close link between

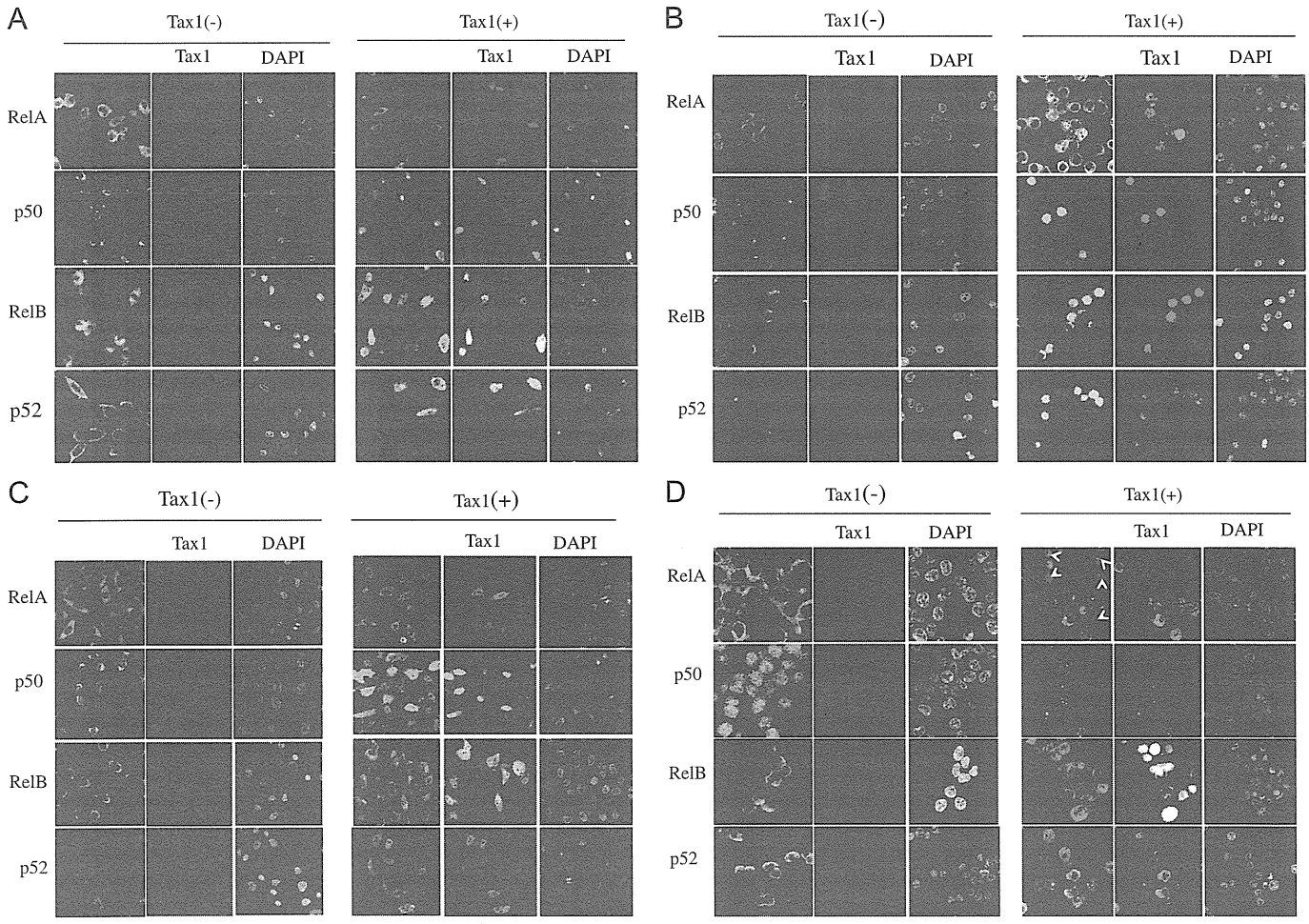

Fig. 5. Expression and function of NF-κB subunits. REF52 (A), Jurkat (B), MG63 (C) and HeLa (D) cells were transfected with or without pMT-2Tax, permealized, stained with the indicated antibodies and observed under a confocal microscope. DAPI was used for nuclear staining. Arrowheads indicate HeLa cells which express RelA in the nucleus without Tax1 expression. For Western blotting, lysates were prepared from REF52 (E) and Jurkat (F) transfected with pMT-2Tax, and MG63 (G) and HeLa (H) cells transfected with pMT-2Tax or cultured with TNFα, electrophoresed and transferred onto membranes. The membranes were treated by ECL system with the indicated antibodies. C23 and β-tubulin were used as marker proteins in nucleic and cytoplasmic fractions, respectively. REF52 cells were cultured with TNFα and examined for IgκB site responses in luciferase reporter assays (I), IκBα phosphorylation in Western blotting (K) and RelA and RelB localization in immunostaining (J). Data are means ± SE. $^{*}P < 0.05$.

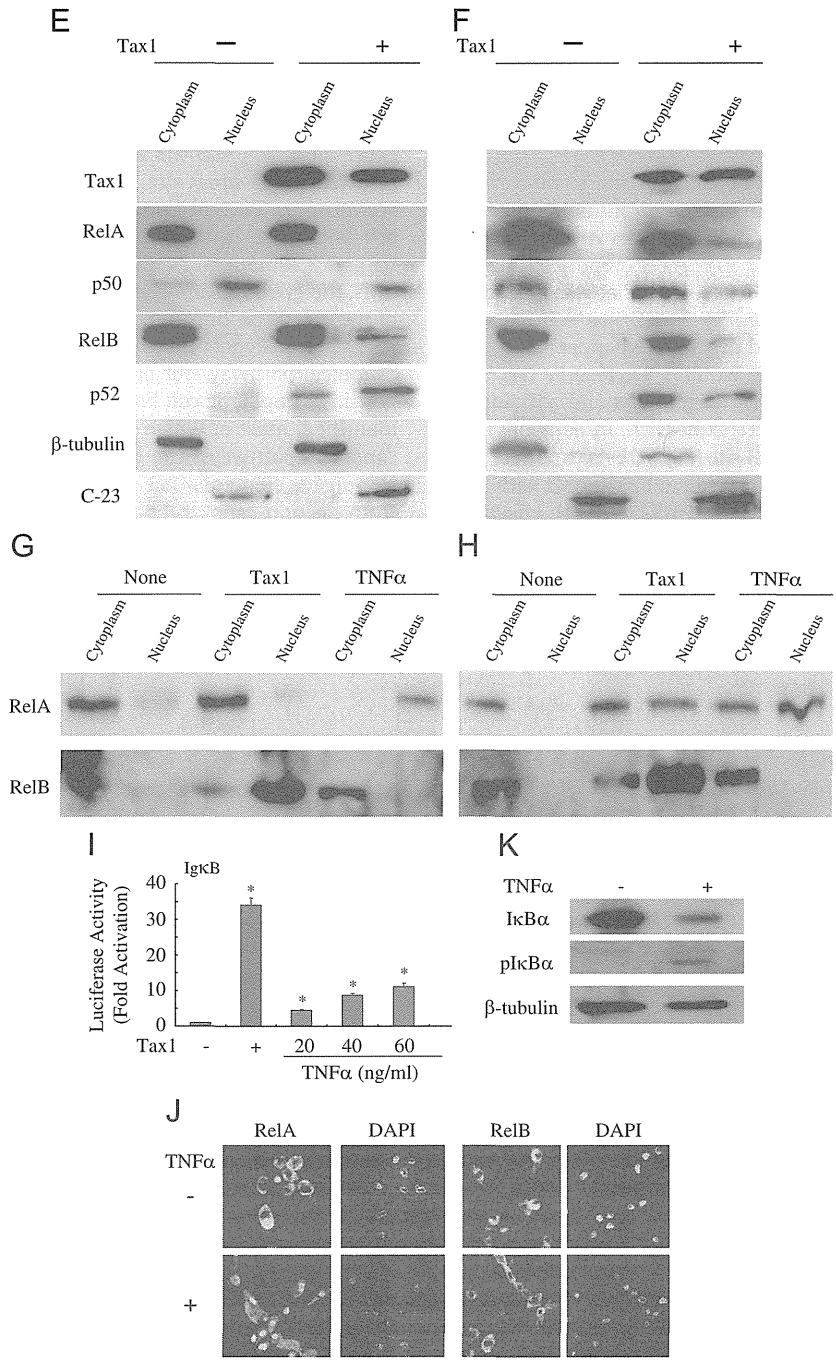

Fig. 5. (*continued*)

Tax1 and malignant transformation (Grossman et al., 1995; Matsuoka and Jeang, 2007; Shoji et al., 2009). In fact, Tax1 mutants lacking the ability to activate NF-κB show poor transforming activity. HTLV-2 Tax2 activates NF-κB similar to Tax1, however malignant transformation by Tax2 has rarely been reported (Higuchi and Fujii, 2009).

In contrast to Tax1, Tax2 immortalizes primary T cells efficiently (our unpublished observations). The efficient immortalization by Tax2 may be attributed to Tax2 specific effects such as activation of nuclear factor of activaed T cells (NF-AT) (Niinuma et al., 2005). We previously demonstrated that Tax1 scarcely induces production of IL-2 in T cells (Mizuguchi et al., 2009). Our results in this study exhibited different activation patterns of the NF-κB binding sites by Tax1 and Tax2; for example, Tax2 activated the IgκB site less extensively than Tax1 in REF52 cells (Fig. 4). Taking account of the poor ability of Tax2 to activate the non-canonical pathway, this is somewhat unexpected. The difference may be a result that NF-AT is activated by Tax2 but not by either Tax1 or Tax1/2, and also the IgκB site may be responsive to NF-AT. Similarly, in Jurkat cells, gpκB response to Tax2 was less than that to Tax1 (Fig. 4). Tax1 activates the canonical and non-canonical pathways in Jurkat cells, inducing full activation of NF-κB. Tax2 and Tax1/2 predominantly activate the canonical pathway, presumably resulting in reduced response of the gpκB site to Tax2, compared with response to Tax1. The different effects of Tax1 and Tax2 on activation of the κB sites may be closely associated with the differences in pathogenesis by infection with HTLV-1 and HTLV-2.

These assumptions may raise the question why the gpκB site is not capable of binding of RelB and p52 in non-hematopoietic cell

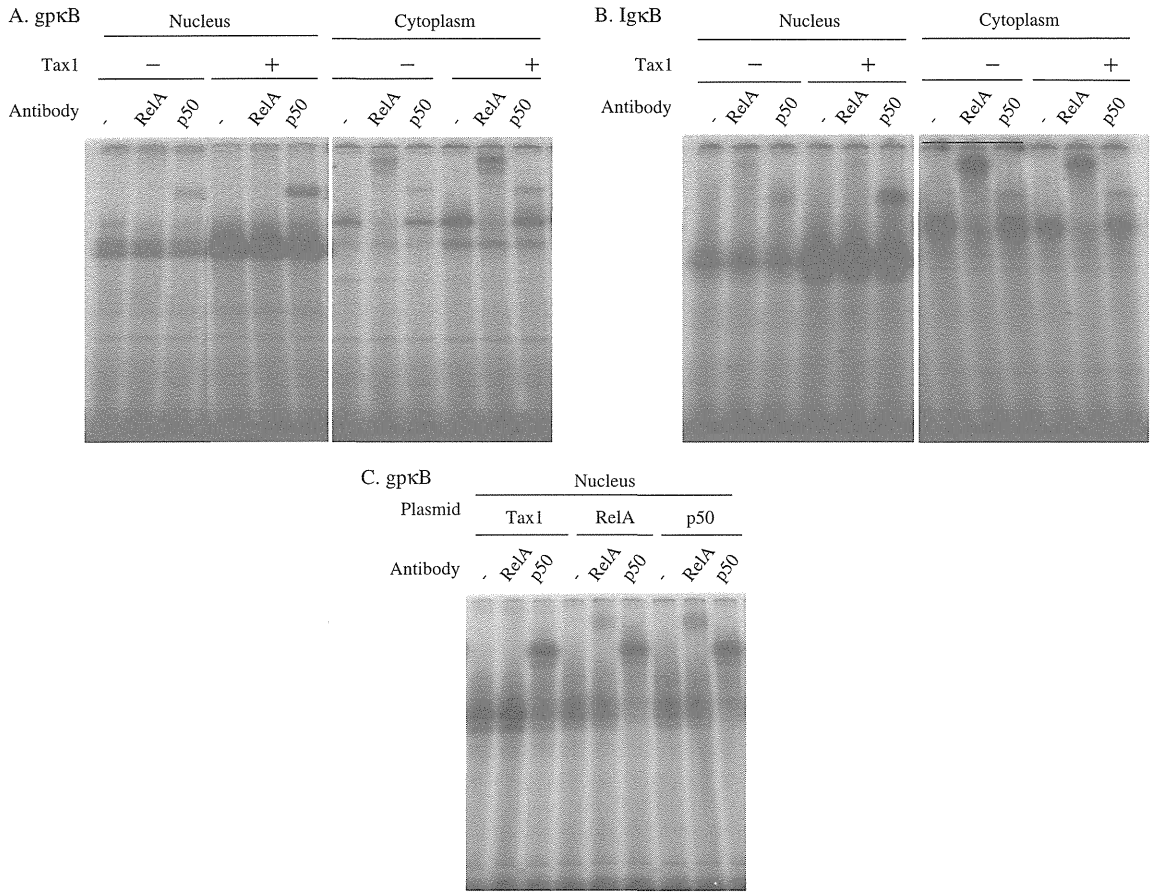

Fig. 6. NF-κB binding to κB sites *in vitro*. The gpκB (A and C) and IgκB (B) sites were used as probes. Probes were labeled and incubated with either nuclear extracts or cytoplasmic extracts prepared from REF52 cells with or without Tax1 expression. Antibodies for RelA and p50 were added to the reaction mixture 1 h prior to the addition of probes. Samples were electrophoresed on polyacrylamide gels and autoradiographed.

lines. It is obvious that Tax1-expressing those cells contained active non-canonical complex RelB/p52, because the IgκB site recruited the RelB/p52 complex (Fig. 7A). However the gpκB site did not show appreciable binding of RelB and p52. At this moment, a solid answer to this question has not been found. Association of RelB and p52 with the gpκB site may be dependent on RelA and p50 binding to the site. This notion may be supported by the result that all four subunits of NF-κB are associated with the gpκB site in Tax1-expressing Jurkat cells (Fig. 7B). Further examination is necessary to clarify this issue.

To gain insight into the mechanism accounting for inactivation of the canonical pathway in non-hematopoietic cell lines, we examined the expression of the canonical pathway subunits RelA and p50. Both molecules were expressed in REF52 cells at a protein level. Although p50 was present in the nucleus and able to bind the gpκB site upon Tax1 expression, RelA was not found in the nucleus even after Tax1 introduction (Figs. 5 and 7). EMSA examination demonstrated complex formation of RelA and p50 with the gpκB site using cytoplasmic lysates, suggesting that the functional complex of RelA and p50 is present in REF52 cells. The gpκB site is capable of RelA/p50 binding. Since Tax1 has been shown to activate the RelA and p50 complex by interaction with IKKγ in the IKK complex (Harhaj et al., 1999; Jin et al., 1999b), we further examined expression of IKKγ by immunostaining with anti-IKKγ antibody. Our observations clearly showed that IKKγ was present in REF52 cells (data not shown). These results imply that an unknown mechanism inhibiting the activation of the canonical pathway complex RelA and p50 may be present in non-hematopoietic cell lines. This mechanism might be related to the process of translocation from the cytoplasm to the nucleus, because RelA was not seen in the nucleus in Tax1 expressing cells.

Cell type-dependent activation of NF-κB by Tax1 is reminiscent of Tax1-mediated activation of the transcription factor E2F. Tax1 activated E2F in hematopoietic cells, however REF52 cells showed little effect of Tax1 on E2F function (Ohtani et al., 2000). Although a cellular factor mediating Tax1-dependent activation of E2F is not known, the Tax1 mutant without the ability to activate NF-κB is also unable to activate E2F (Ohtani et al., 2000). In addition, we observed that Tax2 lacked the ability to activate E2F (our unpublished results). E2F plays critical roles, as a transcription factor, in cell proliferation through progression of the G1 to S phase transition in the cell cycle (Mizuguchi et al., 2011; Ohtani and Nakamura, 2002). Collectively, development of cell transformation by Tax1 may require activation of both the canonical and non-canonical pathways, which are not associated with non-hematopoietic cell lines and Tax2, respectively.

In summary, HTLV-1 Tax1 does not activate the canonical NF-κB pathway in the non-hematopoietic cell lines used in this study and the NF-κB binding site in the OX40L promoter does not respond to the non-canonical pathway in those cells.

Materials and methods

Cell culture

REF52, MG63, HeLa and 293T cells were cultured in Dulbecco's modified Eagle's medium (DMEM) supplemented with 10% fetal

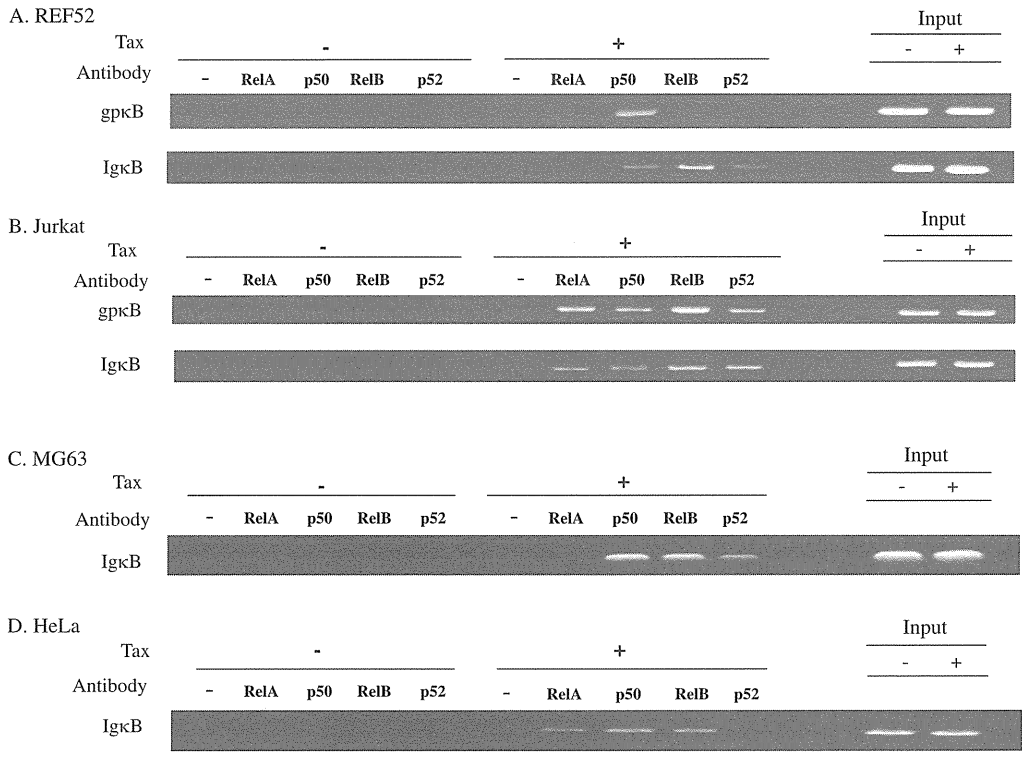

Fig. 7. NF-κB binding to κB sites *in vivo*. Chromatin complexes were prepared from REF52 (A), Jurkat (B), MG63 (C) and HeLa (D) cells transfected with reporter plasmids and pMT-2Tax. After sonication, immunoprecipitation was performed with the antibodies indicated. Precipitated DNA fragments were subjected to PCR with primers specific for the gpκB and IgκB sites in plasmids. The PCR products were 369-bp and 449-bp in length for the gpκB and IgκB sites, respectively.

bovine serum (FBS) with penicillin G (1000 U/ml) and streptomycin (10 μg/ml). Huh7 and HepG2 cells were cultured in DMEM-high glucose (D5796, Sigma-Aldrich) with 10% FBS and antibiotics (Sainz et al., 2009; Wilkening et al., 2003). C-1300 cells were cultured in RPMI1640 medium supplemented with 5% FBS and antibiotics (Fukuhara et al., 1996). Jurkat, K562 and Raji cells were cultured in RPMI1640 with 10% FBS and antibiotics (Karpova et al., 2005; Lozzio and Lozzio,1979; Schneider et al., 1977). TNFα was added to REF52 cell culture for 30 min at a concentration of 40 ng/ml otherwise stated. Cells were cultured at 37 °C in humidified atmosphere with 5% CO_2 in air.

Plasmids

The reporter plasmids used were pIgκB-Luc and pgpκB-Luc carrying three tandem repeats of κB sites in the immunoglobulin light chain (IgκB: 5' –GGGGACTTTCC–3') and gp34 (OX40L) (gpκB: 5'–GGGGAAATTCA–3') genes, respectively, in pGL3-Basic vector (Promega) with the gp34 (OX40L) core promoter (from −31 to +27) (Ohtani et al., 1998). Expression plasmids of NF-κB subunits were R/C CMV RelA for RelA/p65, R/C CMV p50 for p50, R/C CMV RelBM2 for RelB, pCM-p52 for p52, pCn100 for p100 and pEF/c-Rel for c-Rel (Baker et al., 1990; Latimer et al., 1998; Nakayama et al., 1992; Tripathi and Aggarwal, 2006; Yamaoka et al., 1996). The Tax1 expression plasmids pMT-2Tax and pEFneoTax1, and the expression plasmids for wild type Tax2B and a chimeric mutant of Tax1 and Tax2 (Tax1/2) have been described previously (Matsumoto et al., 1997; Shoji et al., 2009). The β-galactosidase expression plasmid pCMV-β-gal was used as an internal control of transfection (Gunning et al., 1987; Matsumoto et al., 1994).

Antibody

Antibodies to NF-κB subunits (RelA, SC-372; p50, SC-114; RelB, SC-19 and p52, SC-848), anti-C23 antibody (H-250), anti-IκBα antibody (SC-371) and anti-β-tubulin antibody (H-235) were purchased from Santa Cruz. Anti-Tax1 mouse monoclonal antibody TAXY-7 is described elsewhere (Tanaka et al., 1991). Anti-phospho-IκBα antibody (5A5) was obtained from Cell Signaling. Fluorescein isothiocyanate (FITC)-conjugated anti-rabbit IgG antibody (eBioscience) and Texas Red-conjugated anti-mouse IgG antibody (Vector) were used for visualization.

Luciferase reporter assay

REF52 and MG63 cells were transfected with 5 μg of plasmid DNA in 2 × HEPES buffered saline with 0.25 M $CaCl_2$ 24 h after cell plating in a 10 cm dish. Jurkat, K562 and Raji cells were transfected with 5 μg of plasmid DNA in DEAE-dextran solution [5 mg/ml in 1 M Tris–HCl (pH 7.4)]. Cells were harvested for reporter assays 48 h post transfection. C-1300, Huh7, HepG2, HeLa and 293T cells were transfected with 1 μg of plasmid DNA using Lipofectamine™ 2000 (Invitrogen) and harvested 24 h after transfection. Luciferase activity was measured with a luminometer (LB 9507, Lumat) using the Luciferase Assay System (Promega) and the activity of luciferase was normalized to β-galactosidase activity which was measured by absorption at 410 nm, or to protein content which was determined by absorption at 750 nm with a spectrophotometer (DU 64, Beckman). Assays were performed at least three times in triplicate. The means ± SE are presented.

Small-interfering RNA (siRNA)

REF52 cells was plated on a 12 well plate and incubated with siRNA (Santa Cruz) for RelB (SC-36403), p52 (SC-36043), RelA (SC-61876) and p50 (SC-156175) at a final concentration of 10 nM in Lipofectamine™ RNAiMAX (Invitrogen) at 37 °C for 6 h. Cells were cultured in medium with 10% FBS and antibiotics for 24 h, transfected with pIgκB-Luc along with pMT-2Tax in Lipofectamine 2000. Cells were further cultured for 24 h and harvested for luciferase activity measurement.

Electrophoretic mobility shift assay (EMSA)

Nuclear and cytoplasmic lysates were prepared from cells transfected with or without the indicated expression plasmids as described (Adachi et al., 1998). From each lysate, 5 μg protein were incubated with [^{32}P]-labeled probes containing κB binding (IgκB and gpκB) sites in DNA-binding buffer [13 mM HEPES (pH 7.8), 8% glycerol, 65 mM NaCl, 1 mM DTT, 0.15 mM EDTA and 1 μg of poly (dI-dC)]. In supershift assays, antibodies (1 μg) were added 1 h before probe addition. The reaction products were separated on 4% polyacrylamide gels in 5 × TBE buffer [450 mM Tris (pH 8.0), 450 mM boric acid and 10 mM EDTA (pH 8.0)] for 4 h at 200 V. Gels were dried and autoradiographed.

Chromatin immunoprecipitation (ChIP) assay

Cells were fixed in 10% formaldehyde solution for 15 min at 37 °C. Crosslinked cells were harvested, lysed in a buffer [50 mM Tris–HCl (pH 8.1), 1% SDS and 5 mM EDTA] containing 1 mM phenylmethylsulfonyl fluoride (PMSF) and sonicated 6 times of 30 s at output 4 of Duty 80 (UD-201, Tomy). The supernatant liquid was collected by centrifugation and incubated with dilution buffer [20 mM Tris–HCl (pH 8.1), 2 mM EDTA, 150 mM NaCl and 1% Triton X-100] containing PMSF with 2 μg of salmon sperm DNA, 20 μl of normal rabbit serum (Dako) and 45 μl of rProtein A Sepharose (GE Health Bio-Science) for 2 h at 4 °C. After rProtein A Sepharose was removed from samples, 2 μg of antibody (anti-RelA, anti-p50, anti-RelB or anti-p52 antibody) was added to each sample and incubated on a rotating platform for 24 h at 4 °C. Salmon sperm DNA (2 μg) and 45 μg of rProtein A Sepharose were added to each sample and incubated for 1 h at 4 °C. DNA fragments were eluted, purified and subjected to PCR with specific primers (IgκB site, forward primer, 5'–TGGAGCGGCCGCAATAAAATA–3', reverse primer, 5'-GGGCGGAGAATGGGCGGAAACT-3' gpκB site, forward primer, 5'-CGGGCCTCTTCGCTATTAG-3' reverse primer, 5'-GCGCCGGGCCTTTCTTTATGTTTT-3'). PCR products were electrophoresed on 2% agarose gels.

Western blotting assay

Cells transfected with or without pMT-2Tax were harvested for preparation of nuclear and cytoplasmic lysates. Cells were lysed with buffer A [10 mM HEPES (pH 7.8), 1.5 mM $MgCl_2$, 10 mM KCl, 0.1% NP-40, 1 mM DTT and 0.5 mM PMSF] and centrifuged to separate nuclei from supernatants. The resultant supernatants were used as sources of cytoplasmic lysates after addition of glycerol and KCl at final concentrations of 20% and 100 mM, respectively. Nuclear lysates were prepared by extraction from nuclei with buffer C [50 mM HEPES (pH 7.8), 420 mM KCl, 0.1 mM EDTA, 5 mM $MgCl_2$, 2% glycerol, 1 mM DTT and 0.5 mM PMSF]. Electrophoresis was performed with 20 μg of protein on 9% polyacrylamide gels. Proteins were blotted into membranes (AE-6667, Atto). Membranes were immunostained and visualized with antibodies using Enhanced Chemi Luminescence (ECL) (Amersham Biosciences).

Immunofluorescence staining

Cells were plated on cover glasses, fixed with 10% paraformaldehyde in PBS, and permeabilized with 0.4% Triton X-100 in PBS. Cells were incubated in 3% bovine serum albumin fraction V in PBS for 30 min and further incubated with mouse anti-Tax1 monoclonal antibody (TAXY-7) at 5 μg/ml for 1 h followed by the addition of Texas Red-conjugated anti-mouse IgG antibody. Anti-RelA, anti-p50, anti-RelB and anti-p52 antibodies were used at 5 μg/ml with FITC-conjugated anti-rabbit IgG antibody. Cells were examined with a laser scanning confocal microscope (FV10i, Olympus).

Statistical analysis

Differences in means between samples and controls were assessed for statistical significance by the student's t-test. Values less than 0.05 are taken statistically significant.

Acknowledgments

We thank J. Inoue and S. Yamaoka for providing NF-κB expression plasmids, and W. Hall for a Tax2 clone. We are grateful to L. Preston for critical reading of the manuscript.

Appendix A. Supporting information

Supplementary data associated with this article can be found in the online version at http://dx.doi.org/10.1016/j.virol.2013.04.032.

References

Adachi, O., Kawai, T., Takeda, K., Matsumoto, M., Tsutui, H., Sakagami, M., Nakanishi, K., Akira, S., 1998. Targeted disruption of the *MyD88* gene results in loss of IL-1- and IL-18-mediated function. Immunity 9, 143–150.

Akagi, T., Ono, H., Shimotohno, K., 1995. Characterization of T cells immortalized by Tax1 of human T-cell leukemia virus type 1. Blood 86, 4243–4249.

Baker, S.J., Markowitz, S., Fearon, E.R., Willson, J.K., Vogelstein, B., 1990. Suppression of human colorectal carcinoma cell growth by wild-type p53. Science 249, 912–915.

Ballard, D.W., Bohnlein, E., Lowenthal, J.W., Wano, Y., Franza, B.R., Greene, W.C., 1988. HTLV-I Tax induces cellular proteins that activate the κB element in the IL-2 receptor α gene. Science 241, 1652–1655.

Baum, P.R., Gayle, R.B., Ramsdell, F., Srinivasan, S., Sorensen, R.A., Watson, M.L., Seldin, M.F., Baker, E., Sutherland, G.R., Clifford, K.N., 1994. Molecular characterization of murine and human OX40/OX40 ligand systems: identification of a human OX40 ligand as the HTLV-1-regulated protein gp34. EMBO J. 13, 3992–4001.

Ben-Neriah, Y., Karin, M., 2011. Inflammation meets cancer, with NF-κB as the matchmaker. Nat. Immunol. 12, 715–723.

Fujii, M., Tsuchiya, H., Chuhjo, T., Akizawa, T., Seiki, M., 1992. Interaction of HTLV-1 Tax1 with p67^{SRF} causes the aberrant induction of cellular immediate early genes through CArG boxes. Genes Dev. 6, 2066–2076.

Fukuhara, S., Mukai, H., Kako, K., Nakamura, K., Munekata, E., 1996. Further identification of neurokinin receptor types and mechanisms of calcium signaling evoked by neurokinins in the murine neuroblastoma C1300 cell line. J. Neurochem. 67, 1282–1292.

Geleziunas, R., Ferrell, S., Lin, X., Mu, Y., Cunningham Jr., E.T., Grant, M., Connelly, M. A., Hambor, J.E., Marcu, K.B., Greene, W.C., 1998. Human T-cell leukemia virus type 1 Tax induction of NF-κB involves activation of the IκB kinase α (IKKα) and IKKβ cellular kinases. Mol. Cell. Biol. 18, 5157–5165.

Giam, C.Z., Jeang, K.T., 2007. HTLV-1 Tax and adult T-cell leukemia. Front. Biosci. 12, 1496–1507.

Grossman, W.J., Kimata, J.T., Wong, F.H., Zutter, M., Ley, T.J., Ratner, L., 1995. Development of leukemia in mice transgenic for the tax gene of human T-cell leukemia virus type I. Proc. Natl. Acad. Sci. USA 92, 1057–1061.

Gunning, P., Muscat, G., Ng, S.Y., Kedes, L., 1987. A human β-actin expression vector system directs high-level accumulation of antisense transcripts. Proc. Natl. Acad. Sci. USA 84, 4831–4835.

Harhaj, E.W., Harhaj, N.S., 2005. Mechanisms of persistent NF-κB activation by HTLV-I Tax. IUBMB Life 57, 83–91.

Harhaj, E.W., Sun, S.C., 1999. IKKγ serves as a docking subunit of the IκB kinase (IKK) and mediates interaction of IKK with the human T-cell leukemia virus Tax protein. J. Biol. Chem. 274, 22911–22914.
Higuchi, M., Fujii, M., 2009. Distinct functions of HTLV-1 Tax1 from HTLV-2 Tax2 contribute key roles to viral pathogenesis. Retrovirology 6, 117.
Higuchi, M., Tsubata, C., Kondo, R., Yoshida, S., Takahashi, M., Oie, M., Tanaka, Y., Mahieux, R., Matsuoka, M., Fujii, M., 2007. Cooperation of NF-κB2/p100 activation and the PDZ domain binding motif signal in human T-cell leukemia virus type 1 (HTLV-1) Tax1 but not HTLV-2 Tax2 is crucial for interleukin-2-independent growth transformation of a T-cell line. J. Virol. 81, 11900–11907.
Hinuma, Y., Nagata, K., Hanaoka, M., Nakai, M., Matsumoto, T., Kinoshita, K.I., Shirakawa, S., Miyoshi, I., 1981. Adult T-cell leukemia: antigen in an ATL cell line and detection of antibodies to the antigen in human sera. Proc. Natl. Acad. Sci. USA 78, 6476–6480.
Ishii, N., Takahashi, K., Soroosh, P., Sugamura, K., 2010. OX40-OX40 ligand interaction in T-cell-mediated immunity and immunopathology. Adv. Immunol. 105, 63–98.
Jin, D.Y., Giordano, V., Kibler, H., Nakano, H., Jeang, K.T., 1999. Role of adapter function in oncoprotein-mediated activation of NF-κB. Human T-cell leukemia virus type I Tax interacts directly with IκB kinase γ. J. Biol. Chem. 274, 17402–17405.
Karpova, M.B., Schoumans, J., Ernberg, I., Henter, J.I., Nordenskjöld, M., Fadeel, B., 2005. Raji revisited: cytogenetics of the original Burkitt's lymphoma cell line. Leuk. Res. 19, 159–161.
Latimer, M., Ernst, M.K., Dunn, L.L., Drutskaya, M., Rice, N.R., 1998. The N-terminal domain of IκBα masks the nuclear localization signal(s) of p50 and c-Rel homodimers. Mol. Cell. Biol. 18, 2640–2649.
Lenzmeier, B.A., Giebler, H.A., Nyborg, J.K., 1998. Human T-cell leukemia virus type 1 Tax requires direct access to DNA for recruitment of CREB binding protein to the viral promoter. Mol. Cell. Biol. 18, 721–731.
Lozzio, B.B., Lozzio, C.B., 1979. Properties and usefulness of the original K-562 human myelogenous leukemia cell line. Leuk. Res. 3, 363–370.
Matsumoto, K., Shibata, H., Fujisawa, J.I., Inoue, H., Hakura, A., Tsukahara, T., Fujii, M., 1997. Human T-cell leukemia virus type 1 Tax protein transforms rat fibroblasts via two distinct pathways. J. Virol. 71, 4445–4451.
Matsumoto, K., Akashi, K., Shibata, H., Yutsudo, M., Hakura, A., 1994. Single amino acid substitution (58Pro→Ser) in HTLV-1 tax results in loss of ras cooperative focus formation in rat embryo fibroblasts. Virology 200, 813–815.
Matsuoka, M., Jeang, K.T., 2007. Human T-cell leukaemia virus type 1 (HTLV-1) infectivity and cellular transformation. Nat. Rev. Cancer 7, 270–280.
Miura, S., Ohtani, K., Numata, N., Niki, M., Ohbo, K., Ina, Y., Gojobori, T., Tanaka, Y., Tozawa, H, Nakamura, M., Sugamura, K., 1991. Molecular cloning and characterization of a novel glycoprotein, gp34, that is specifically induced by the human T-cell leukemia virus type I transactivator p40 Tax. Mol. Cell. Biol. 11, 1313–1325.
Mizuguchi, M., Hara, T. and Nakamura, M., Roles of HTLV-1 Tax in leukemogenesis of human T-cells. Intech, T-Cell Leukemia, Rijeka, Croatia, 2011, pp. 51–64.
Mizuguchi, M., Asao, H., Hara, T., Higuchi, M., Fujii, M., Nakamura, M., 2009. Transcriptional activation of the interleukin-21 gene and its receptor gene by human T-cell leukemia virus type 1 Tax in human T-cells. J. Biol. Chem. 284, 25501–25511.
Nakayama, K., Shimizu, H., Watanabe, T., Okamoto, S., Yamamoto, K., 1992. A lymphoid cell-specific nuclear factor containing c-Rel-like proteins preferentially interacts with interleukin-6 κB-related motifs whose activities are repressed in lymphoid cells. Mol. Cell. Biol. 12, 1736–1746.
Niinuma, A., Higuchi, M., Takahashi, M., Oie, M., Tanaka, Y., Gejyo, F., Tanaka, F., Sugamura, K., Xie, L.P., Green, L., Fujii, M., 2005. Aberrant activation of the interleukin-2 autocrine loop through the nuclear factor of activated T cells by nonleukemogenic human T-cell leukemia virus type 2 but not by leukemogenic type 1 virus. J. Virol. 79, 11925–11934.
Ohtani, K., Nakamura, M., 2002. Molecular mechanism of Tax-mediated cell growth of human T lymphocytes. Gann Monogr. Cancer Res. 50, 50–67.
Ohtani, K., Tsujimoto, A., Tsukahara, T., Numata, N., Miura, S., Sugamura, K., Nakamura, M., 1998. Molecular mechanisms of promoter regulation of the gp34 gene that is trans-activated by an oncoprotein Tax of human T cell leukemia virus type I. J. Biol. Chem. 273, 14119–14129.
Ohtani, K., Iwanaga, R., Arai, M., Huang, Y., Matsumura, Y., Nakamura, M., 2000. Cell type-specific E2F activation and cell cycle progression induced by the oncogene product Tax of human T-cell leukemia virus type I. J. Biol. Chem. 275, 11154–11163.
Osame, M., Usuku, K., Izumo, S., Ijichi, N., Amitani, H., Igata, A., Matsumoto, M., Tara, M., 1986. HTLV-I associated myelopathy, a new clinical entity. Lancet 1, 1031–1032.
Poiesz, B.J., Ruscetti, F.W., Gazdar, A.F., Bunn, P.A., Minna, J.D. and Gallo, R.C., 1980. Detection and isolation of type C retrovirus particles from fresh and cultured lymphocytes of a patient with cutaneous T-cell lymphoma. Proc. Natl. Acad. Sci. USA 77, 7415–7419.
Qu, Z., Xiao, G., 2011. Human T-cell lymphotropic virus: a model of NF-κB-associated tumorigenesis. Viruses 3, 714–749.
Ross, T.M., Pettiford, S.M., Green, P.L., 1996. The tax gene of human T-cell leukemia virus type 2 is essential for transformation of human T lymphocytes. J. Virol. 70, 5194–5202.
Schneider, U., Schwenk, H.U., Bornkamm, G., 1977. Characterization of EBV-genome negative "null" and "T" cell lines derived from children with acute lymphoblastic leukemia and leukemic transformed non-Hodgkin lymphoma. Int. J. Cancer 19, 621–626.
Sainz, B., TenCate, V., Uprichard, S.L., 2009. Three-dimensional Huh7 cell culture system for the study of Hepatitis C virus infection. Virol. J. 6, 103.
Shoji, T., Higuchi, M., Kondo, R., Takahashi, M., Oie, M., Tanaka, Y., Aoyagi, Y., Fujii, M., 2009. Identification of a novel motif responsible for the distinctive transforming activity of human T-cell leukemia virus (HTLV) type 1 Tax1 protein from HTLV-2 Tax2. Retrovirology 6, 83.
Tanaka, Y., Inoi, T., Tozawa, H., Yamamoto, N., Hinuma, Y., 1985. A glycoprotein antigen detected with new monoclonal antibodies on the surface of human lymphocytes infected with human T-cell leukemia virus type-I (HTLV-I). Int. J. Cancer 36, 549–555.
Tanaka, Y., Yoshida, A., Tozawa, H., Shida, H., Nyunoya, H., Shimotohono, K., 1991. Production of a recombinant human T-cell leukemia virus type-I transactivator (tax1) antigen and its utilization for generation of monoclonal antibodies against various epitopes on the tax1 antigen. Int. J. Cancer 48, 623–630.
Tripathi, P., Aggarwal, A., 2006. NF-κB transcription factor: a key player in the generation of immune response. Curr. Sci. 90, 519–527.
Wilkening, S., Stahl, F., Bader, A., 2003. Comparison of primary human hepatocytes and hepatoma cell line HepG2 with regard to their biotransformation properties. Drug Metab. Dispos. 31, 1035–1042.
Xiao, G., Cvijic, M.E., Fong, A., Harhaj, E.W., Uhlik, M.T., Waterfield, M., Sun, S., 2001. Retroviral oncoprotein Tax induces processing of NF-κB2/p100 in T cells: evidence for the involvement of IKK. EMBO J. 20, 6805–6815.
Yamaoka, S., Inoue, H., Sakurai, M., Sugiyama, T., Hazama, M., Yamada, T., Hatanaka, M., 1996. Constitutive activation of NF-κB is essential for transformation of rat fibroblasts by the human T-cell leukemia virus type I Tax protein. EMBO J. 15, 873–887.
Yoshida, M., Miyoshi, I., Hinuma, Y., 1982. Isolation and characterization of retorovirus from cell lines of human adult T-cell leukemia and its implication in the disease. Proc. Natl. Acad. Sci. USA 79, 2031–2035.
Yoshida, M., 2001. Multiple viral strategies of HTLV-1 for dysregulation of cell growth control. Ann. Rev. Immunol. 19, 475–496.
Zhao, L.J., Giam, C.Z., 1992. Human T-cell lymphotropic virus type I (HTLV-I) transcriptional activator, Tax, enhances CREB binding to HTLV-I 21-base-pair repeats by protein-protein interaction. Proc. Natl. Acad. Sci. USA 89, 7070–7074.

Regular Article

LYMPHOID NEOPLASIA

HTLV-1 Tax oncoprotein stimulates ROS production and apoptosis in T cells by interacting with USP10

Masahiko Takahashi,[1] Masaya Higuchi,[1] Grace Naswa Makokha,[1] Hideaki Matsuki,[1] Manami Yoshita,[1] Yuetsu Tanaka,[2] and Masahiro Fujii[1]

[1]Division of Virology, Niigata University Graduate School of Medical and Dental Sciences, Niigata, Japan; and [2]Department of Immunology, Graduate School and Faculty of Medicine, University of the Ryukyus, Nishihara, Okinawa, Japan

Key Points

- Interaction of HTLV-1 Tax with USP10 reduces arsenic-induced stress granule formation and enhances ROS production.
- USP10 controls sensitivities of leukemia cell lines to arsenic-induced apoptosis.

Human T-cell leukemia virus type 1 (HTLV-1) is the etiological agent of adult T-cell leukemia (ATL), and the viral oncoprotein Tax plays key roles in the immortalization of human T cells, lifelong persistent infection, and leukemogenesis. We herein identify the ubiquitin-specific protease 10 (USP10) as a Tax-interactor in HTLV-1–infected T cells. USP10 is an antistress factor against various environmental stresses, including viral infections and oxidative stress. On exposure to arsenic, an oxidative stress inducer, USP10 is recruited into stress granules (SGs), and USP10-containing SGs reduce reactive oxygen species (ROS) production and inhibit ROS-dependent apoptosis. We found that interaction of Tax with USP10 inhibits arsenic-induced SG formation, stimulates ROS production, and augments ROS-dependent apoptosis in HTLV-1–infected T cells. These findings suggest that USP10 is a host factor that inhibits stress-induced ROS production and apoptosis in HTLV-1–infected T cells; however, its activities are attenuated by Tax. A clinical study showed that combination therapy containing arsenic is effective against some forms of ATL. Therefore, these findings may be relevant to chemotherapy against ATL. (*Blood.* 2013;122(5):715-725)

Introduction

Environmental stresses, such as hypoxia, heat shock, UV irradiation, and arsenite, induce several alterations in cells, such as DNA damage and accumulation of misfolded proteins, the short- and long-term consequences of which include survival of cells with aberrant DNA and protein alterations, inflammation, aging, and carcinogenesis. On the other hand, cells activate several defense mechanisms to protect against these outcomes. For instance, cells transiently induce the formation of cytoplasmic RNA granules designated as stress granules (SGs).[1,2] SGs have several antistress functions. The stresses induce translational arrest, leading to polysome disassembly, and SGs transiently store translationally inactive messenger RNAs released from polysomes and promote the translation of stress-repairing proteins, such as heat shock proteins. In addition, SGs inhibit reactive oxygen species (ROS) production and ROS-dependent apoptosis,[3] and in the meantime, cells repair altered DNA and remove misfolded proteins. Therefore, SGs play critical roles in protecting against stress-induced alterations in cells.

Viral infections have also been shown to induce the formation of SGs in host cells, although some viruses encode proteins that inhibit the formation of SGs.[4] For instance, the poliovirus-encoded protease 3C protein prevents SG formation via protease-dependent cleavage of Ras-GTPase–activating protein-binding protein 1 (G3BP1),[5] which is essential for SG assembly.[6] In addition, the NS1 encoded by the influenza A virus inhibits SG formation by preventing the activation of protein kinase that initiates a phosphorylation cascade leading to SG formation after viral infection.[7] On the basis of these observations, SGs are proposed to be involved in innate immunity against viral infections, and the inhibition of SG formation stimulates viral replication and production and augments inflammation and tissue damage.[8]

Human T-cell leukemia virus type 1 (HTLV-1) is an etiologic agent of adult T-cell leukemia (ATL).[9] Accumulation of genetic and epigenetic aberrations in HTLV-1–infected cells is a crucial step for ATL development, as only 5% of HTLV-1–infected individuals go on to have ATL at an average of 40 years after infection. Indeed, ATL cells have multiple DNA alterations, such as mutations of cellular oncogenes and tumor suppressor genes. HTLV-1 encodes the Tax oncoprotein, which plays crucial roles in the immortalization of virus-infected T cells, accumulation of gene mutations in infected cells, and leukemogenesis.[9,10] To perform such pleiotropic functions, Tax exhibits a variety of activities, including transcriptional activation of a number of cellular genes via the actions of transcription factors nuclear factor κB (NF-κB), cAMP response element binding/activating transcription factor (CREB/ATF), and AP-1 and inactivation of the tumor suppressor gene p53.[11-13] Notably, Tax also inhibits SG formation[14]; however, its significance in HTLV-1 pathogenicity remains to be clarified.

Ubiquitin-specific protease 10 (USP10) is a component of SGs that plays critical roles in several SG-mediated activities. USP10 is not essential for SG formation; however, its knockout in mouse

Submitted March 27, 2013; accepted June 3, 2013. Prepublished online as *Blood* First Edition paper, June 17, 2013; DOI 10.1182/blood-2013-03-493718.

The online version of this article contains a data supplement.

The publication costs of this article were defrayed in part by page charge payment. Therefore, and solely to indicate this fact, this article is hereby marked "advertisement" in accordance with 18 USC section 1734.

embryonic fibroblasts (MEFs) reduces SG formation, augments ROS production, and enhances ROS-dependent apoptosis.[3] In our current study, we identified USP10 as a novel binding partner of Tax protein. The activities of Tax mutants and knockdown of USP10 indicated that Tax, by interacting with USP10, inhibits SG formation and stimulates ROS production. Accumulating evidence indicates that aberrant ROS production is a factor promoting gene mutations that cause malignancy.[15] Therefore, the present findings indicate that USP10 is a host factor that inhibits ROS-induced aberration of HTLV-1–infected T cells, including genetic mutations. Notably, a previous clinical study showed that combination therapy containing arsenic trioxide, an anhydrous form of arsenite, exhibits promising effects against some forms of ATL.[16] Our results revealed that knockdown of USP10 augments arsenite-induced ROS-dependent apoptosis in HTLV-1–infected T cells. Therefore, USP10 controls the sensitivity of ATL cells to arsenic and is hence a novel target for chemotherapy against ATL.

Methods

Reagents and antibodies

The following reagents were purchased from the indicated companies: sodium arsenite (Wako Pure Chemical Industries), arsenic trioxide (Sigma-Aldrich), puromycin (Calbiochem) and *N*-acetylcysteine (NAC; Sigma-Aldrich). Arsenic trioxide was first dissolved in 1.0 N of NaOH and was then diluted with phosphate-buffered saline (PBS). The following antibodies were used in this study at the indicated dilutions: anti-USP10 (1:2000; Bethyl Laboratories), anti-HA (1:2000; Cell Signaling Technology), anti-G3BP1 (1:2000; BD Transduction Laboratories), anti-poly(A)-binding protein 1 (PABP1) (1:1000; Santa Cruz, 1:500; Abcam), anti-Tax (Taxy-7)[17] (1:1000), and anti-α-tubulin (1:1000; Oncogene).

Coimmunoprecipitation and western blot analysis

The coimmunoprecipitation and western blot analysis were performed as described previously.[3]

Immunofluorescence analysis

An immunofluorescence analysis was performed as described previously.[3] The images were analyzed with a fluorescence microscope (BZ-8000; KEYENCE). More than 300 cells in 3 random fields were analyzed using staining with SG markers, G3BP1 and USP10. The SG (%) was calculated as the ratio of SG-positive cells relative to the total number of cells.

Detection of ROS

Cellular ROS level was measured as described previously.[3] The 5-chloromethyl-2′,7′-dichlorodihydrofluorescein diacetate (CM-H_2DCFDA) fluorescence in each cell was quantified using a fluorescent analysis software package (BZ-II analyzer; KEYENCE). More than 400 cells in 4 random fields were analyzed, and the data were presented as the mean fluorescence intensity (DCFDA-F).

Quantitative determination of apoptosis

The level of apoptosis was measured according to 2 methods. First, the cells were stained with propidium iodide, and the sub-G1 DNA content was measured using flow cytometry. Second, cells cultured on coverslips in 6-well plates were fixed with 4% formaldehyde in PBS and were permeabilized with 0.1% Triton X-100 in PBS. The fixed cells were stained with Hoechst33258. After Hoechst33258 staining, the number of cells that exhibited condensed nuclei was counted using a fluorescence microscope. More than 300 cells in 3 random fields were analyzed per sample.

Statistical analysis

The data were analyzed using the unpaired Student *t* test and are presented as the mean ± standard deviation (SD). Information including "Cell lines and culture conditions," "Plasmid constructs," and the "Establishment of stable USP10-knockdown cell lines using lentiviral transduction" is provided in the supplemental Methods, available on the *Blood* Web site.

Results

Tax interacts with USP10

Cytotoxic T lymphoblast cell (CTLL)-2 is a mouse interleukin (IL)-2–dependent T-cell line. Tax transforms CTLL-2 cells from IL-2–dependent growth into IL-2–independent growth, and its activity is much higher than that of nonleukemogenic HTLV-2 Tax2.[18,19] Studies of chimeric Tax proteins including Tax2 have revealed that the C-terminal PDZ domain-binding motif (PBM) in Tax, which is missing in Tax2, is a factor responsible for the high transforming activity of CTLL-2.[18,19] To obtain information on how Tax PBM augments the Tax-induced transformation of CTLL-2, we isolated several Tax-binding proteins in CTLL-2 cell lysates using glutathione *S*-transferase fusion proteins of Tax vs TaxΔC with deletion of PBM (M.H. and M.F., unpublished observations). One such Tax-binding protein is USP10. To establish the interaction between Tax and USP10 in mammalian cells, plasmids encoding Tax as well as USP10 with a hemagglutinin (HA) epitope (HA-USP10) were transiently expressed in 293T cells, and the cell lysates were immunoprecipitated with anti-HA antibodies. The anti-HA antibody coprecipitated HA-USP10 with Tax (Figure 1A). Conversely, anti-Tax coprecipitated HA-USP10 with Tax (Figure 1B). Unexpectedly, USP10 also interacted with the Tax PBM mutant TaxΔC (Figure 1B), indicating that PBM is not essential for the interaction between Tax and USP10. In addition, Tax formed a complex with USP10 in HTLV-1–infected T cells (Figure 1C). A total of 7 HTLV-1–positive and 3 HTLV-1–negative T-cell lines constitutively expressed USP10 as well as 2 USP10-binding proteins, G3BP1[20] and PABP1,[21] and the levels of these factors did not correlate with that of Tax (Figure 1D). An immunofluorescence analysis visualized endogenous and exogenous USP10 in the cytoplasm, where some proteins colocalized with Tax (Figures 1E and 6A; as represented by arrows). Taken together, these results indicate that Tax interacts with USP10 in HTLV-1–infected T cells, and these molecules partly colocalize in the cytoplasm.

To delineate the domain of Tax that is responsible for the interaction with USP10, we examined the interactions between Tax mutants and USP10. Three of the mutants, TaxSH-1, TaxSH-2, and $Tax^{62\text{-}353}$, exhibited minimal interaction with USP10 (Figure 2A-B). TaxSH-1 and TaxSH-2 have point mutations at Pro-58 to Ser and Leu-205 to Arg, respectively. $Tax^{62\text{-}353}$ has an *N*-terminal deletion from amino acids 1 to 61, containing the zinc finger region. Therefore, both the *N*-terminal region and the central region of Tax are required for interaction with USP10. On the other hand, TaxM22 and Tax703 demonstrated equivalent USP10-binding activity to wild-type (WT) Tax and have point mutations at Gly-137 and Leu-138 and at Leu-319 and Leu-320, respectively (Figure 2A-B).

To identify the domain of USP10 responsible for the interaction with Tax, plasmids encoding various USP10 mutants were constructed (Figure 2C). An immunoprecipitation analysis of 293T cells showed that the deletion of amino acids 727 to 798 of the C-terminal region of USP10 prominently reduced binding with Tax, whereas the